

**PROPERTIES OF ELECTRODEPOSITED METALLIC  
SYSTEMS (SCHOTTKY DIODES) ON  
SEMICONDUCTOR SUBSTRATES**

**MSc Thesis**

**in**

**Engineering Physics**

**University of Gaziantep**

**Supervisor**

**Prof. Dr. Ömer Faruk BAKKALOĞLU**

**by**


**Özden DEMİRCİOĞLU**

**Jan 2011**


T.C.  
UNIVERSITY OF GAZIANTEP  
GRADUATE SCHOOL OF  
NATURAL & APPLIED SCIENCES  
ENGINEERING PHYSICS

Name of the thesis: Properties of Electrodeposited Metallic Systems (Schottky Diodes) on Semiconductor Substrates  
Name of the student: Özden DEMİRCİOĞLU  
Exam date:14.01.2011

Approval of the Graduate School of Natural and Applied Sciences

  
Prof. Dr. Ramazan KOÇ  
Director

I certify that this thesis satisfies all the requirements as a thesis for the degree of Master of Science.

  
Prof. Dr. A. Necmeddin Yazıcı  
Head of Department

This is to certify that we have read this thesis and that in our consensus/majority opinion it is fully adequate, in scope and quality, as a thesis for the degree of Master of Science.

  
Prof. Dr. Ömer Faruk BAKKALOĞLU  
Supervisor

Examining Committee Members

signature

Prof. Dr. Ömer Faruk BAKKALOĞLU

Doc. Dr. Metin BEDİR

Doc. Dr. Hanifi ÇANAKÇI



## ABSTRACT

### PROPERTIES OF ELECTRODEPOSITED METALLIC SYSTEMS (SCHOTTKY DIODES) ON SEMICONDUCTOR SUBSTRATES

DEMİRCİOĞLU, Özden

MSc Thesis, Engineering of Physics, University of Gaziantep

Supervisor: Prof. Dr. Ömer Faruk BAKKALOĞLU

January 2011, 54 pages

In this study, by using n-type Si substrate with (100) orientation, 150 nm thickness and 10-20  $\Omega\text{m}$  resistivity and chromium doped, thin film Schottky diode system (Cr/n-Si SBHs which is electrochemically formed on n-type Si) is constructed and characterized. In the electrical characterization of this diodes, the current – voltage (I-V) and the capacitance – voltage (C-V) measurements are done.

The basic diode parameters such as ideality factor ( $n$ ) and barrier height ( $\Phi_b$ ) were consequently extracted from electrical measurements. It has been shown that the ideality factors increased and barrier heights decreased with the decreasing temperatures, on the basis of the thermionic emission (TE) theory.

The homogeneity or the uniformity of the Schottky BH is an issue with important implications on the theory of Schottky barrier formation and important ramifications for the operation of Schottky barrier diodes and contacts. Thus, provided semiconductor substrate is well characterized, the homogeneous Schottky BH may be obtained even from the I-V characteristics of one contact. For this purpose, Cr/n-type Si SBHs with a doping density of about  $1.25 \times 10^{15} \text{ cm}^{-3}$  is prepared and the linear region with large BHs is used. The electrical characteristics of Cr/n-type structures were investigated in the wide temperature range (80-320 K) by steps of 20 K.

Key words: Silicon, Schottky barrier diodes, Electrodeposition Method.

## ÖZET

### ELEKTRODEPOLAMA YÖNTEMİYLE YARIİLETKEN ÜZERİNE METAL (Cr-Chromium) DEPOLAYARAK ELEKTRİKSEL ÖZELLİKLERİNİN İNCELENMESİ

DEMİRCİOĞLU, Özden

Yüksek Lisans Tezi, Fizik Mühendisliği, Gaziantep Üniversitesi

Danışman: Prof. Dr. Ömer Faruk BAKKALOĞLU

Ocak 2011, 54 sayfa

Bu çalışmada, (100) doğrultusunda büyütülmüş, 150 nm kalınlıklı ve 10-20  $\Omega\text{m}$  öz dirençli ve n tipi Silisyum kullanarak, elektrodepolama yöntemiyle oluşturduğumuz Cr/n-Si Schottky diyotların elektriksel özellikleri incelendi. Bu diyotların elektriksel karakteristikleri, akım-voltaj ( $I$ - $V$ ) ve kapasitans-voltaj ( $C^2$ - $V$ ) ölçümlerinin yardımıyla belirlendi.

Elektrodepolama yöntemiyle oluşturduğumuz Cr/n-Si diyotun bariyer yükseklikleri ve idealite faktörleri sıcaklığa bağlı olarak incelenip lineer ilişki yardımıyla belirlendi. TE teoremine göre; idealite faktörünün sıcaklık azaldıkça arttığını, bariyer yüksekliğinin ise sıcaklık arttıkça arttığı gösterildi.

Schottky bariyer yüksekliğinin oluşum teorisinde, Schottky bariyer yüksekliğinin özdeşliği ve homojenliği önemli bir konudur ve Schottky bariyer diyot ve kontakların oluşumunda önemli bir daldır. Böylece yarı-iletken madde iyi karakterize edilip homojen Schottky bariyer yüksekliği, tek bir kontakın  $I$ - $V$  karakteristiğinden de elde edilebilir. Bu amaçla, yaklaşık  $1.25 \times 10^{15} \text{ cm}^{-3}$  katkı yoğunluklu Cr/n-tipi Si SBDlar hazırlandı ve BHLı lineer bölge kullanıldı. Cr/n-tipi Si yapılarının elektriksel karakteristikleri sıcaklığa bağlı olarak 80 ile 320  $^{\circ}\text{K}$  arasında 20  $^{\circ}\text{K}$  arttırarak incelendi.

**Anahtar kelimeler:** Silisyum, Schottky bariyer diyot, Elektodepolama yöntemi

## **ACKNOWLEDGEMENTS**

This study is advanced by the supervision of Prof. Dr. Ömer Faruk BAKKALOĞLU. I would like to express my great thanks to him for his guidance , advice , suggestion and encouragement.

The co-operation and support of Prof. Dr. Abdülmecit TÜRÜT (Atatürk University, ERZURUM) were very valuable who gave me the opportunity of being investigated our substances in the laboratories of Atatürk University.

My gratitude also goes to Dr. Şükrü KARATAŞ (University of Kahramanmaraş Sütçü İmam) for his valuable discussion.

My special thanks go to my family for their understanding.

## CONTENTS

	Page
ABSTRACT .....	i
ÖZET .....	ii
ACKNOWLEDGEMENTS .....	iii
CONTENTS .....	iv
LIST OF FIGURES .....	vi
LIST OF TABLES .....	viii
LIST OF SYMBOLS .....	ix
CHAPTER 1: GENERAL INTRODUCTION .....	1
CHAPTER 2: SCHOTTKY BARRIER CONTACTS .....	3
2.1 Introduction .....	3
2.2 Metal/n-type Semiconductor Contacts .....	3
2.2.1 Schottky (Rectifier) Contacts .....	3
2.3 Metal/p-type Semiconductor Contacts .....	5
2.3.1 Schottky (Rectifier) Contacts .....	5
2.3.2 The Effects on The Scottky Barrier Height .....	7
2.3.3 Current Transmision With The Thermionic Emission in the Schottky Diodes .....	8
2.3.4 Ideality Factor on Schottky Diodes .....	12
2.3.5 Cheung Functions and Determining Characteristics of Schottky Diodes .....	15
2.3.6 The Schottky Capacity in the Metal-Semiconductor Schottky Diodes ..	17
2.4 Ohmic Contacts .....	20
CHAPTER 3: EXPERIMENTAL PROCEDURE .....	23
3.1 Introduction .....	23

3.2 Electrodeposition Method.....	23
3.2.1 Experimental set up of Electrodeposition System.....	26
3.3 Growth Mechanism of the Thin Films by Electrodeposition Method.....	27
3.4 Preparation of the Substrate.....	27
3.5 Production of Schottky Diodes.....	28
3.6 The development of the Chromium Layer on the n-type Silicon Wafer .....	29
CHAPTER 4: MEASUREMENTS AND RESULTS.....	30
4.1 Measurement Techniques.....	30
4.1.1 Current-Voltage Measurement.....	31
4.1.2 Capacitance- Voltage Measurement.....	32
CHAPTER 5: RESULTS AND DISCUSSION.....	33
5.1 Current-Voltage Measurement Results of the Schottky Diodes.....	33
5.2 The $T_0$ effect.....	38
5.3 Inhomogeneous barrier analysis.....	39
5.4 Norde's function for the series resistance calculation.....	44
CHAPTER 6: CONCLUSIONS.....	47
REFERENCES.....	48

## LIST OF FIGURES

	page
Figure 2.1 a)The energy band diagrams of the metal and the semiconductor before the contact b)The energy band diagram after the contact	4
Figure 2.2 Energy band diagram for metal and p-type semiconductor a)before contact b)after contact at thermal equilibrium.	6
Figure 2.3 The energy band diagram of the image decreasing effect in the metal/n-type semiconductor Schottky diode under forward bias.	8
Figure 2.4 (a) potential distribution (b)Charge distribution of the metal/p-type rectifying contacts dependent to state.	17
Figure 2.5 ( $\phi_m < \phi_s$ ) for this situation the energy band diagram of metal/n-type semiconductor ohmic contact.	20
Figure 2.6 a) The barrier before doping. b) The barrier after doping. Black dots show us the conducting electrons.	21
Figure 2.7 Decreasing of the Schottky barrier at the M-S junction in the case of an n-type graded-gap semiconductor. The band gap in the graded-gap semiconductor changes from $E_{g1}$ to $E_{g2}$ .Black dots show the conducting electrons.	21
Figure 2.8 Energy band diagram for metal p-type semiconductor in thermal equilibrium after contact.	22
Figure 3.1 Electrolytic cell for the deposition of copper from copper sulphate solution.	24
Figure 3.2 Electrical double layer.	25
Figure 3.3 The diagram of the oven and control unit for the ohmic contact thermal process.	28



Figure 4.1 Keithley 487 Picoammeter/Voltage Source.	30
Figure 4.2 Structure and sign convection of a metal-semiconductor junction.	31
Figure 5.1 Current-voltage characteristics of the Cr/ <i>n</i> -Si Schottky contact at various temperatures.	34
Figure 5.2 Temperature dependence of the ideality factor and barrier heights for Cr/ <i>n</i> -Si Schottky contact.	37
Figure 5.3 Experimental capacitance-voltage characteristics of a typical Cr/ <i>n</i> -Si Schottky contact in the temperature range of 80-320K.	37
Figure 5.4 Plot of $nkT$ as a function of $kT$ showing the $T_0$ anomaly from $n = n_o + (T_0/T)$ . The dashed line shows the ideal behaviour, $n = 1$ . The open triangles are the experimental data in the temperature range of 80–320 K in Fig. 1. The value of the slope and the $T_0$ are shown in the figure.	38
Figure 5.5 Conventional activation energy ( $\ln(I_0/T^2)$ versus $1/kT$ ) plot (the open squares) and ( $\ln(I_0/T^2)$ versus $1/nkT$ ) plot (the open triangles) for Cr/ <i>n</i> -Si Schottky contact.	40
Figure 5.6 The barrier height $\Phi_{ap}$ (the open triangles) obtained from $I$ - $V$ measurements as a function of inverse temperature and the inverse ideality factor $1/n_{ap}$ (the open squares) versus inverse temperature ( $1/2kT$ ) plot for Cr/ <i>n</i> -Si Schottky contact.	41
Figure 5.7 Modified activation energy ( $\ln(I_0/T^2) - q^2 \sigma_o^2 / 2k^2T$ versus $1/kT$ ) plots for Cr/ <i>n</i> -Si Schottky contact according to two Gaussian distributions of barrier heights. The plots for zero-bias standard deviation $\sigma_s$ equal to 0.109 V and 0.072 V are shown by open triangles and open squares, respectively. The straight lines 1 and 2 indicate the best fitting of the data in the temperature ranges 200-320 K and 80-180 K, respectively.	43
Figure 5.8 $F(V)$ versus $V$ plot of the Cr/ <i>n</i> -Si Schottky contact at various temperature.	45
Figure 5.9 Temperature dependence of the series resistance from the Norde's functions of Cr/ <i>n</i> -Si Schottky contact.	46

## LIST OF TABLES

	page
Table 5.1 Temperature dependent values of various experimental parameters obtained from $I$ - $V$ and $C$ - $V$ measurements of the Cr/ $n$ -Si Schottky contact.	35

## LIST OF SYMBOLS

$A$	The effective diode area ( $\text{cm}^2$ )
$A^*$	The Richardson constant
$C$	The Schottky capacitance
$E_C$	Energy of the conduction band
$E_f$	Fermi energy
$f(E)$	The Fermi-Dirac (probability) distribution function
$g_c(E)$	The density of state in the conductivity band
$H$	The coercive field
$h$	The Planck constant
$I_0$	Saturation current
$J$	Current density
$k$	The Boltzmann constant
$m_n^*$	The effective mass of the $n$ -type semiconductor
$n$	Ideality factor (forward slope factor, depends upon metal-semiconductor interface)
$N_D$	The donor concentration of $n$ -type semiconductor substrate
$R_S$	Series resistance
$T$	The absolute temperature
$V_a$	Applied voltage
$V_{bi}$	Built in potential
$V_d$	Diffusion potential
$\Phi_{bn}$	The barrier height of a metal-semiconductor Schottky diode
$\Phi_{b0}$	Asymptotic value of $\Phi_{bn}$ at zero electric field
$\Delta\Phi$	The Schottky barrier lowering

$\Phi_m$	The work function of metal
$\Phi_s$	The work function of semiconductor
$X_s$	The electron affinity of the semiconductor
$\epsilon_s$	The dielectric constant of the semiconductor
$\epsilon_0$	The dielectric constant of vacuum
$\rho$	Resistivity
$\rho(x)$	The space charge density
$\Psi(x)$	The potential function
$Q$	In the semiconductor the charge density for unit area

## CHAPTER 1

### GENERAL INTRODUCTION

The metal-semiconductor (MS) contact is one of the most widely used rectified contacts in the electronic industry [1,2]. The current transport across a Schottky contact is the interest of material science and device physics. Due to the technological importance of metal-semiconductor structures, a full understanding of their current-voltage (I-V) and capacitance-voltage(C-V) characteristics are of great interest[3-7]. Ideal metal-semiconductor contacts are considered to be intimate, abrupt, laterally homogeneous, and then the continuum of the metal-induced gap states (MIGS) determines their barrier height[8-11].The electronic properties of a Schottky contact are characterized by its barrier height and ideality factor parameters.The most important feature characterizing Schottky barrier diodes(SBDs) is its barrier height (BH).When metal makes contact with a semiconductor , a barrier is formed at the metal semiconductor interface. This barrier is responsible for controlling the current conduction as well as its capacitance behaviour.Schottky contacts with low barrier height find applications in devices operating at cryogenic temperatures such as infrared detectors, sensors in thermal imaginig, microwave diodes,gates of transistors and infraredand nuclear particle detectors[12,13].The Schottky barrier height (SBH) is likely to be a function of the interface atomic structure, and the atomic inhomogenities at metal-semiconductor(MS) interface which are caused by grain boundaries,multiple phases, facets, defects, a mixture of different phases,etc.[14,15].The SBH controls the electron transport across the M-S interface and is at vital importance to the successful operation of any semiconductor device.Most studies of Schottky diodes formed on n-type Si were limited to the determination of the SBH at room temperature by measuring either the C-V characteristics or the forward I-V characteristics of the diodes [16,17].Important additional information can be gained from the temperature dependence of forward I-V characterisatics.It allows the identification of the different conduction mechanism modes across the metal-semiconductor interface and the study of different effects,such as barrier inhomogeneities and surface states density, on carrier transport at metal semiconductor Schottky contacts [18-24].

Si is an important integral for very –large-scale integration(VLSI)circuits in many applications.Among the different methods available for metallization of Si surfaces,vacuum deposition is the usual metallization method.However, the electrodepositon is an advantageous alternative to the common expensive physical technologies for the metallization of semiconductors.This technique can especially be preferred for the deposition of metals with high melting points such as Cr, Ni, Co, etc., which are very difficult to evaporate by physical techniques [25-30]. Moreover,it provides the possibility of depositing film structures different from those being produced from the vapor phase.

The analysis of the I-V characteristics of SBDs based on thermionic emission theory usually reveals an abnormal decrease in the BH  $\phi_b$  and an increase in the ideality factor  $n$  with decreasing temperature [22,31-33].The decrease in barrier height at low temperatures in fact leads to nonlinearity in the activation energy( $\ln(I_0/T^2)$ ) versus  $1/T$ ) plot.These findings can not be explained adequately by incorporating interface states or an interfacial oxide layer, tunneling, and image force lowering or generation recombination effects [22,34].The ‘‘To-effect’’ is advanced to explain the variation of ideality factor with temperature [34,35]. This requires the  $nT$  versus  $T$  plot to be a straight line.Lately , the nature and origin of the decrease with temperature have been satisfactorily explained in some studies [4,10,11,12,22,24,32,34 and 36] recently by incorporating the concept of barrier inhomogenities and introducing a thermionic emission mechanism with Gassuian distrubution function of the barrier heights.

In this study,the I-V and C-V characteristics of Cr Schottky contacts on n-type Si substrate by electrodepositon technique were measured over the temperature range of 80-320 K by steps of 20 K.The analysis of the forward-bias characteristics of the devices based on TE mechanism have revealed an abnormal decrease of  $\phi_b$  and increase of  $n$  with decreasing temperatures, and these changes become effective especially at low temperatures.The temperature dependent barrier characteristics of the Cr/n- type Si Schottky contacts were interpreted by assuming double-Gaussian spatial distribution of BHs.Furthermore, the series resistance effect was observed from the I-V characteristics.Therefore,Norde’s function was used to determine some contact parameters such as the barrier height and the value of series resistance of the Cr/n-type Si Schottky contact.

## CHAPTER 2

### SCHOTTKY BARRIER CONTACTS

#### 2.1 Introduction

A Schottky Barrier diode is a contact between a metal and a semiconductor which has rectifying properties. To consider the characteristic parameters of Schottky diodes, a contact which is proper to investigate the properties of Schottky diodes is needed. When the contact is done between metal and semiconductor, the transporting of charge is proceeded between materials until the chemical potential in the semiconductor reaches equilibrium with the Fermi energy level of the metal. When the metal's work function is bigger than the semiconductor in n-type contacts, a rectifier contact occurs. When the semiconductor's work function is bigger than the metal in n-type contacts, an ohmic contact occurs.

#### 2.2 Metal/n-type Semiconductor Contacts

##### 2.2.1. Schottky (Rectifier) Contacts

A Schottky barrier is a metal-semiconductor junction which has rectifying characteristics, suitable for use as a diode. The largest differences between a Schottky barrier and a p-n junction are its typically lower junction voltage, and decreased (almost nonexistent) depletion width in the metal.

In general, when two conductors (e.g. metals) are connected to each other, the charge transporting continues until the electrochemical potentials equalize. A depletion region is formed because of new charge distribution in the contact region and this region is a dipolar region within a conductive, doped semiconductor where the charge carriers have diffused away, or have been forced by an electric field. This depletion region occurs due to the fact that two conductors (metals) are connected to each other. The metal-metal contact where electrons are moved freely in both directions is called ohmic contact. This phenomenon occurs not only in a two conductor system but also in a semiconductor and metal system. When a metal and a semiconductor are connected to each other, either ohmic or rectifier contact can be formed. In a rectifier contact, electrons are moved easily in one direction (forward bias), however, in the

opposite direction, electrons can't pass through easily because of the potential barrier (reverse bias). This situation is related to the energy-band diagram of metal-semiconductor system. To explain this event, we can take into consideration a metal and n-type semiconductor contact. Assume that all donor atoms are ionized. The work function of metal is  $\phi_m$ , the work function of semiconductor is  $\phi_s$ , and the electron affinity of semiconductor is  $\chi_s$  and also  $\phi_m > \phi_s$ .

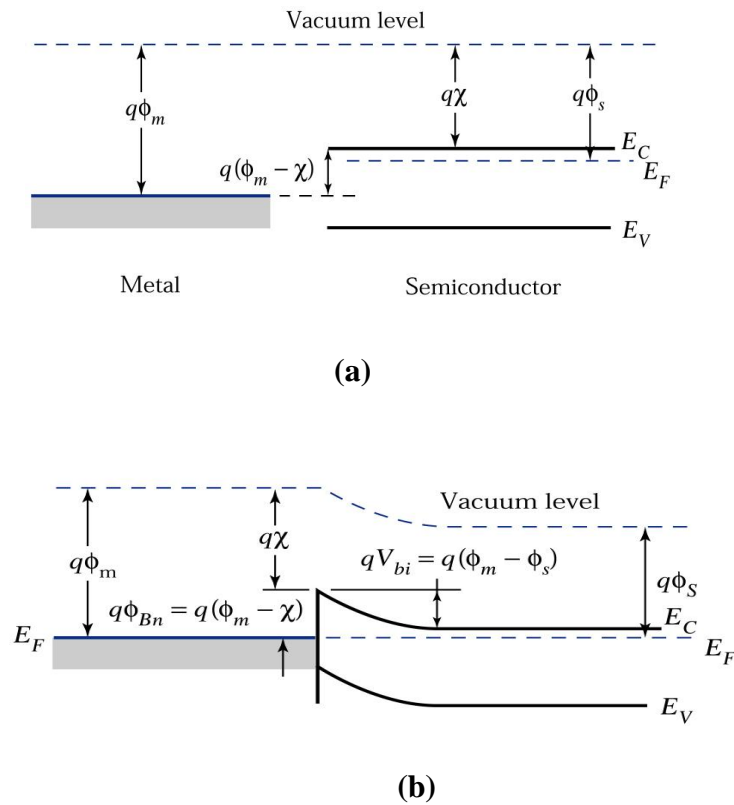


Figure 2.1:(a)The energy band diagrams of the metal and the semiconductor before the contact (b)The energy band diagram after the contact.

Before the formation of contact, as it can be seen in Figure 2.1(a), the Fermi level of the semiconductor is higher than the metal's Fermi level by the amount of  $\phi_m - \phi_s$ . When the electrons flow from semiconductor to metal after the contact, they leave ionized donor atoms behind. This continues until the chemical potential is reached in equilibrium with the Fermi energy of the metal. In another word, the Fermi level of semiconductor is lowered by  $\phi_m - \phi_s$  as seen in Figure 2.1(b). As a result of depletion region, a potential barrier develops at the surface. And this barrier's height for the semiconductor is  $\phi_m - \phi_s$  and the barrier height for the metal is  $\phi_m - \chi_s$ . We can



write this barrier height in terms of the diffusion potential  $eV_{\text{dif}} = e(\phi_m - \phi_s)$ . When electrons flow from conduction band to metal, they come across the potential barrier. Because the positive charge location in the semiconductor side of the contact is at rest, the surface level of the contact is called ‘space charge level’. Because of the potential barrier in the contact, the surface level is also called as barrier level. The thickness of the surface charge level ( $d$ ) depends on i) the concentration of the ionized donor atoms and ii) the value of the diffusion potential. When some electrons in metal and semiconductor gain enough thermal energy to exceed the potential barrier, the leakage current ( $I_0$ ) takes place in opposite directions and in equal amounts across the contact. If a voltage of  $-V$  is applied to the semiconductor side, the barrier height for the electrons that will flow from metal to semiconductor doesn’t change, and therefore the flow of the electrons does not also change. But in the semiconductor region, the conduction band level increases by  $eV$  and therefore the barrier height for the electrons that will flow from semiconductor to metal decreases by  $eV$ . Consequently, the current flow from metal to semiconductor increases by a factor of  $\exp(eV/kT)$ , the net current is then

$$I = I_0 \left[ \exp\left(\frac{eV}{kT}\right) - 1 \right] \quad (1.1)$$

The net current ( $I$ ) is positive and this situation is called forward bias ( $V \gg kT/e$ ).

If a voltage of  $+V$  is applied to the semiconductor side, the conduction band decreases by  $eV$  and the potential barrier of the semiconductor also increases by  $eV$ . Therefore the net current approaches to  $-I_0$  and this situation is called reverse bias ( $V \ll kT/e$ ).

## 2.3 Metal/p-type Semiconductor Contacts

### 2.3.1. Schottky (Rectifier ) Contact

When a metal and a semiconductor are connected to each other, the charge transporting continues until the electrochemical potentials equalize. In this section, the word of semiconductor refers to p-type semiconductor. In a metal-semiconductor contact, if charge carriers (holes or electrons) can flow in one side easier than the other side, this is called rectifier contact. Thereby, the current passes through easier in one direction.  $\phi_m$  is the work function of metal,  $\phi_s$  is the work function of semiconductor. If the work function of metal is smaller than the work function of the

semiconductor, i.e. ( $\phi_m < \phi_s$ ), the contact is rectifier. If the work function of metal is bigger than the work function of semiconductor, i.e. ( $\phi_m > \phi_s$ ), the contact is ohmic.

Assume that  $\phi_m < \phi_s$ , and at room temperature all acceptor atoms are ionized. Before the contact is formed, the Fermi level of the semiconductor is lower than the Fermi level of the metal by the value of  $\phi_s - \phi_m$  in Figure 2.2(a), after the formation of contact, the electrons flow from the metal side to the p-type semiconductor until thermal equilibrium is reached in Figure 2.2(b). As a result of this, the holes in the semiconductor region become negatively ionized because of the flow of the electrons. The negatively charged acceptor atoms are dispersed within the thickness ( $d$ ) of a region which is called the space charge surface (or region). When the energy level of the semiconductor is increased at the surface, the barrier height becomes  $eV_{diff} = e(\phi_s - \phi_m)$  for holes in the semiconductor.  $V_{diff}$  is the diffusion potential. The barrier height for holes in the metal region is  $e\phi_{bn} = E_s - \phi_m$ .

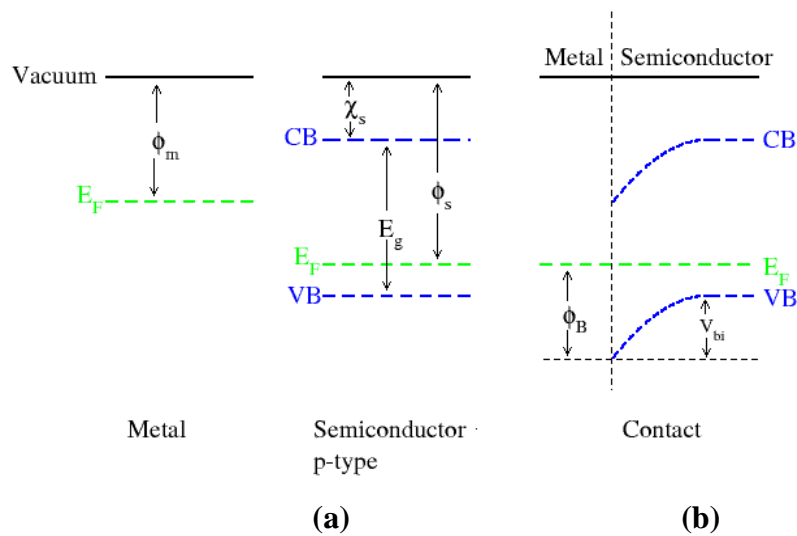


Figure:2.2 Energy band diagram for metal and p-type semiconductor a)before contact b)after contact at thermal equilibrium

Some holes can pass through into the metal after gaining enough thermal energy to exceed the potential barrier, in the same way some holes in metal can pass through into the semiconductor. Thus, there will be equal, opposite two currents ( $I_0$ ) which exceed from barrier through contact. If a positive potential ( $+V$ ) is applied to the semiconductor, there is no change in transporting holes from left side to the right side, but the number of holes flowing from right side to the left side will increase by a factor of  $\exp(eV/kT)$ . Hence, the energy level in the semiconductor decreases by

eV. Therefore, the potential barrier decreases by eV for the holes flowing from right side (semiconductor) to the left side (metal). As a result, if the current from right to the left is assumed to be positive (the current which is constituted by the holes flowing from semiconductor to the metal), the net current will be;

$$I = I_0 \left( \exp \left( \frac{eV}{kT} \right) - 1 \right) \quad (1.1)$$

This contact is called rectifier (Schottky) contact.

### 2.3.2. The Effects on The Schottky Barrier Height

The barrier height for an ideal metal-semiconductor contact is equal to  $\Phi_{Bn} = \phi_m - \chi_s$ . In this equation;  $\phi_m$  is the work function of the metal,  $\chi_s$  is the electron affinity (the electron affinity is defined as the energy difference labelled as  $\chi$  between the bottom of the conduction band and vacuum level.). Some effects can make deviations in the Schottky Barrier Height (SBH) that is written as  $\Phi_{Bn} = \phi_m - \chi_s$ . One of them, the emission current in the cathode increases with rising in the field forces. This effect is also known as Schottky effect. And it relates with the work function of the cathode and depends on the surface field force. An electron in the dielectric region at a distance  $x$  creates an electric field. And this field line will be the same with an image charge  $+e$  which is perpendicular to the metal's surface to inside. The force effect on the electron that brings about the influence of Coulomb and the image charge is called as the image force and expressed as:

$$F = \frac{-e^2}{4\pi\epsilon_s(2x)^2} = -eE \quad (2.1)$$

The potential is ;

$$-\phi(x) = + \int_x^\infty E dx = \int_x^\infty \frac{e}{4\pi\epsilon_s 4(x)^2} dx = \frac{-e}{16\pi\epsilon_s x} \quad (2.2)$$

where  $x$  is the integral variable and for  $x = \infty$ , we accepted the potential as zero. When the external electric field is zero, the potential is equal to the equation 2.2. If the external field is different from zero, then equation will be

$$\phi(x) = \frac{-e}{16\pi\epsilon_s x} - Ex \quad (2.3)$$

The equation (2.2) will lose its validity for the small values of  $x$  and when  $x \rightarrow 0$ , the potential  $\phi(x) \rightarrow \infty$ . The second term in the equation expresses the decreasing in value of potential barrier cause of external field. This decreasing in the potential barrier is known as Schottky effect or the image lowering with the image force.

The decreasing in the Shottky barrier  $\Delta\phi$ ,

$$\frac{d[e\phi(x)]}{dx} = 0 \quad (2.4)$$

Using the equation (2.4), from this condition we can obtain the maximum barrier  $X_m$  as;

$$X_m = \sqrt{\frac{e}{16\pi\epsilon_s E}} \quad (2.5)$$

### **2.3.3. Current Transmision With The Thermionic Emission in the Schottky Diodes**

The electron transmission over the potential barrier in the Shottky diodes is explained with Termionic Emission Theory. The emission of carriers because of thermal energy from a hot surface is known as Thermionic Emission. For metal-semiconductor Schottky diodes, the Thermionic Emission Theory is based on the transmission of charge carriers because of thermal energy exceeding the potential barrier from metal to semiconductor or from semiconductor to metal.

In Schottky diodes, the current transport is provided by majority carriers. For metal/n-type semiconductor, the majority carrierrs are electrons and for metal/p-type semiconductor, holes are majority carriers. While the thermionic emission theory is forming it is assumed that the potential barrier of the Schottky contact is bigger than the energy of  $kT$  and the carrier collision in the depletion region is very small for applying the Maxwell-Boltzman approximation.

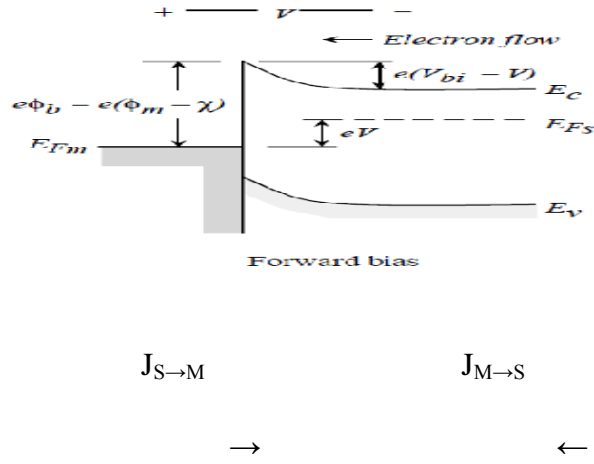


Figure 2.3 The energy band diagram of the image decreasing effect in the metal/n-type semiconductor Schottky diode under forward bias.

Where  $J_{S \rightarrow M}$  is the current density from semiconductor to metal and  $J_{M \rightarrow S}$  is the current density from metal to semiconductor.  $J_{S \rightarrow M}$  is the current density in the +x direction and it is a function of electrons concentration which have enough velocity to exceed the potential barrier. So that;

$$J_{S \rightarrow M} = e \int_{E_x}^{\infty} v_x dx \quad (2.6)$$

where that  $E_x$  is the minimum energy needed for the thermionic emission in the metal,  $v_x$  is the velocity in the drift direction. The increasing concentration of electrons is given;

$$dn = g_c(E) f(E) d(E) \quad (2.7)$$

Here  $g_c(E)$  is the density of state in the conduction band and  $f(E)$  is the Fermi-Dirac distribution function. For the electron concentration, the Maxwell-Boltzmann approximation can be written as;

$$dn = \frac{4\pi(2m_n^*)^{3/2}}{h^3} \sqrt{E - E_c} \exp\left[\frac{-(E - E_f)}{kT}\right] dE \quad (2.8)$$

Here if  $(E - E_c)$  is accepted as a kinetic energy of free electrons, then it can be written as

$$\frac{1}{2} m_n^* v^2 = E - E_c \quad (2.9)$$

$$dE = m_n^* v dv \quad (2.10)$$

and

$$\sqrt{E - E_c} = v \sqrt{\frac{m_n^*}{2}} \quad (2.11)$$

Using these results, if the equation (2.8) is arranged again, we can get the equation (2.12)

$$dn = 2 \left[ \frac{m_n^*}{h} \right]^3 \exp\left(\frac{-e\phi_n}{kT}\right) \exp\left(\frac{-m_n^* v^2}{kT}\right) 4\pi v^2 dv \quad (2.12)$$

This equation (2.12) gives us the number of electrons which change the velocity between  $v$  and  $v + dv$ . If the velocity is separated to its component, it must be like  $v^2 = v_x^2 + v_y^2 + v_z^2$ . So that using this information;

$$J_{S \rightarrow M} = 2e \left( \frac{m_n^*}{h} \right)^3 \exp\left(\frac{-e\phi_n}{kT}\right) \int_{-\infty}^{\infty} v_x \exp\left(\frac{m_n^* v_x^2}{2kT}\right) dv_x \int_{-\infty}^{\infty} \exp\left(\frac{-m_n^* v_y^2}{2kT}\right) dv_y \int_{-\infty}^{\infty} \exp\left(\frac{-m_n^* v_z^2}{2kT}\right) dv_z \quad (2.13)$$

Otherwise for minimum velocity  $v_{0x}$  ;

$$\frac{1}{2} m_n^* v_{0x}^2 = e(V_{bi} - V_a) \quad (2.14)$$

Here  $v_{0x}$  is the minimum velocity to exceed the potential barrier in the electron movement of x direction. In this situation, for that condition  $v_x \rightarrow v_{0x}$ ,  $\alpha = 0$ . Nevertheless, the equation is written as  $v_x dv_x = \left(\frac{2kT}{m_n^*}\right)$ . In the equation (2.13), the parameters can be change with variables.

$$\frac{-m_n^* v_x^2}{2kT} \equiv \alpha^2 + \frac{e(V_{bi} - V_a)}{kT} \quad (2.15i)$$

$$\frac{-m_n^* v_y^2}{2kT} \equiv \beta^2 \quad (2.15ii)$$

$$\frac{m_n^* v_z^2}{2kT} \equiv \gamma^2 \quad (2.15iii)$$

If this expressions are used in the equation (2.13);

$$J_{S \rightarrow M} = J_{x \rightarrow \infty} = 2e \left( \frac{m_n^*}{h} \right)^3 \left( \frac{2kT}{m_n^*} \right)^2 \exp\left(\frac{-e\phi_n}{kT}\right) \exp\left[\frac{e(V_{bi}-V_a)}{kT}\right] x \int_0^\infty \alpha \exp(-\alpha^2) da \int_{-\infty}^\infty -\beta^2 \int_{-\infty}^\infty -\gamma^2 d\gamma$$
(2.16)

If this last (2.16) expression is integrated;

$$J_{S \rightarrow M} = \left( \frac{4\pi e m_n^* k^2}{h^3} \right) T^2 \exp\left[\frac{-e(\phi_n + V_a)}{kT}\right] \exp\left(\frac{eV_a}{kT}\right)$$
(2.17)

or

$$J_{x \rightarrow \infty} = \left( \frac{4\pi e m_n^* k^2}{h^3} \right) T^2 \exp\left[\frac{-e\phi_{Bn}}{kT}\right] \exp\left[\frac{eV_a}{kT}\right]$$
(2.18)

As seen figure 2.5;  $\phi_n + V = \phi_{bn}$  and when the applied voltage is equal to 0 (zero),  $J_{M \rightarrow S}$  and  $J_{S \rightarrow M}$  will be the same. So that ;

$$J_{M \rightarrow S} = \left( \frac{4\pi e m_n^* k^2}{h^3} \right) T^2 \exp\left[\frac{-e\phi_{B0}}{kT}\right]$$
(2.19)

The net current density is equal to  $J = J_{S \rightarrow M} - J_{M \rightarrow S}$ . In other clearer expression for the net current density is ;

$$J = \left[ A^* T^2 \exp\left(\frac{-e\phi_{Bn}}{kT}\right) \right] \left[ \exp\left(\frac{eV_a}{kT}\right) - 1 \right]$$
(2.20)

where  $A^*$  is the Richardson constant for thermionic emission and it equals ;

$$A^* = \frac{4\pi e m_n^* k^2}{h^3}$$
(2.21)

For general expression the net current density in the equation 2.20 will be like as ;

$$J = J_0 \left[ \exp\left(\frac{eV_a}{kT}\right) - 1 \right]$$
(2.22)

where  $J_0$  is known as reverse saturation current density and it expresses as ;

$$J_0 = A^* T^2 \exp\left(\frac{-e\phi_{Bn}}{kT}\right)$$
(2.23)

When the Schottky barrier height is decreased with the image force and defined  $\phi_{bn} = \phi_{b0} - \Delta\phi$ , then equation (2.23) can be written as

$$J_0 = A^*T^2 \exp\left(\frac{-e\phi_{Bn}}{kT}\right) \exp\left(\frac{e\Delta\phi}{kT}\right) \quad (2.24)$$

$\Delta\phi$  change in the barrier height will be increased with increasing reverse bias voltage or in electrical region [37].

### 2.3.4 Ideality Factor on Schottky Diodes

According to Bardeen model, when a semiconductor and a metal are connected, the states of interfaces are localized between the surface of semiconductor and the layer of insulator. Thus, if there is no electrical field into metal or semiconductor, the intensity of the electric field on the interfaces layer is related to the charges on metal's surface and interfaces. According to the Gauss Law

$$\varepsilon_i E_i = Q_{ss} = -Q_m \quad (2.25)$$

can be written. In here;  $E_i$  is the intensity of electric field on interface layer. In generally, there is an electric field in the Schottky barrier and this electric field is important how to affect of the barrier height. If there is an electric field  $E_s$  into the semiconductor, in this condition the Gauss law can be written as;

$$V_i = \frac{\delta}{\varepsilon_i} (\varepsilon_s E_{max} + Q_{ss}) \quad (2.26)$$

In here that;  $V_i$  is the decreasing potential on interface layer and  $E_{max}$  is the maximum value of the  $E_s$ . The ideality factor "n" is analyzed due to the interface parameters (the density of interfaces and the thickness of the interfaces) and dependent on the applied voltage [38-40]. In this view, primarily all interfaces condition in equilibrium with the metal must be considered. If there are a depletion region in semiconductor and interface layers, the applied potential V can be written as;

$$V = V_i + V_s \quad (2.27)$$

In here that  $V_s$  is the changing of potential due to depletion region. If we consider the equation of 2.20, this expression will be ;



$$J = \left[ AA^* T^2 \exp\left(\frac{-q\phi_b}{kT}\right) \right] \left[ \exp\left(\frac{qV}{kT}\right) - 1 \right] \quad (2.28)$$

If the logarithm of this expression (2.28) is taken and then the derivation with respect to V is performed, the equation will be

$$\frac{d \ln I}{dV} = \frac{1}{I} \frac{dI}{dV} = \frac{q}{kT} \left\{ 1 - \frac{d\phi_b}{dV} + \left[ \exp\left(\frac{qV}{kT}\right) - 1 \right]^{-1} \right\} \quad (2.29)$$

In the forward bias condition, the slope of linear side in the graph of  $\ln I - V$  gives us the ideality factor. So the expression of the ideality factor is

$$n = \frac{q}{kT} \frac{dV}{d \ln I} = \frac{1}{(1-\beta)} \quad (2.30)$$

In here  $\beta = d\phi_b/dV$  so that for the ideality factor

$$\frac{1}{n} = 1 - \frac{d\phi_b}{dV} \quad (2.31)$$

The Schottky barrier height is dependent on the electric field in the depletion region so the effective barrier height  $\Phi_e$  is considered instead of  $\Phi_b$ . The expression of the effective barrier height is

$$\Phi_e = \Phi_{b,0} + \left( \frac{d\Phi_e}{dV} \right) V = \Phi_{b,0} + \beta \quad (2.32)$$

where  $d\Phi_e/dV$  is the changing of the effective barrier height due to voltage bias. Again as a result of equations (2.31 and 2.32),  $\beta$  can be written as  $\beta = d\Phi/dV$  and if we consider this expression, the equation 2.28 can be written again as

$$I = I_0 \exp\left(-\frac{\beta qV}{kT}\right) \left[ \exp\left(\frac{qV}{kT}\right) - 1 \right] \quad (2.33)$$

The saturation current  $I_0$

$$I_0 = AA^*T^2 \exp\left(\frac{-q\Phi_{b,0}}{kT}\right) \quad (2.34)$$

If  $d\Phi/dV$  is constant, the ideality factor is constant. If the ideality factor  $n > 1$ , this does not show us only the applied voltage decreases in the depletion region but it also show us the sharing with interface layers, depletion region and the whole body resistance.

Now, when the expression of 2.31 and the equation  $(d\Phi_b/dV = d\Phi/dV) = (dV_i/V)$  are considered and we take a derivation of the equation 2.26 with respect to the applied voltage,

$$\left(1 - \frac{1}{n}\right) = \frac{dV_i}{V} = \frac{\delta}{\epsilon_i} \left( \epsilon_s \frac{dE_{max}}{V} + \frac{dQ_{ss}}{V} \right) \quad (2.35)$$

If we use the equation 2.27,

$$\frac{dE_{max}}{dV} = \frac{dE_{max}}{dV_s} \left(1 - \frac{dV_i}{dV}\right) = \frac{1}{nw} = \frac{1}{w} \frac{dV_s}{dV} \quad (2.36)$$

and

$$\frac{dQ_{ss}}{dV} = \frac{dQ_{sa}}{dV_i} \frac{dV_i}{V} = -qN_{sa} \left(1 - \frac{1}{n}\right) \quad (2.37)$$

Where “w” is the thickness of the depletion region and  $w = (2\epsilon_i V_d / qN_d)^{1/2}$ .

$Q_{sa}$  is the charge density of interfaces which is in equilibrium with metal,

$N_{sa}$  is the density of states of interfaces,

$N_d$  is the concentration of the donor atoms,

$V_d$  is the diffusion potential.

The equation 2.37 gives us the change in states which are occupied in equilibrium with metal and it is determined by  $dV_i$  which is the changing states due to the Fermi energy level of metal. Thus we can write  $(dQ_{sa}/dV_i) = -qN_{sa}$  and if we substitute the equation 2.36 and 2.37 into 2.35;

$$\left(1 - \frac{1}{n}\right) = \frac{\delta}{\varepsilon_i} \left[ \frac{\varepsilon_s}{L_{nw}} - qN_{sa} \left(1 - \frac{1}{n}\right) \right] \quad (2.38)$$

can be obtained and from this expression we can get the equation 2.39

$$n = 1 + \frac{\delta \varepsilon_s}{w(\varepsilon_s + \delta q N_{sa})} \quad (2.39)$$

This equation is valid for the equilibrium states is achieved between metal and interfaces. When the states of interfaces are equilibrium in the semiconductor, the charges density of interfaces  $Q_b$  and the density of states  $N_{sb}$  are taken and we can get a new expression for this situation;

$$\frac{dQ_{ss}}{dV} = \frac{dQ_{sb}}{dV_s} \frac{dV_s}{dV} = \frac{qN_{sb}}{n} \quad (2.40)$$

This expression gives us the change in the interfaces which are occupied in equilibrium with semiconductor and it is determined by  $dV_s$  which is the change in states due to the Fermi energy level of semiconductor. Thus, we can write  $(dQ_{sb}/dV_s) = qN_{sb}$  and if we substitute the equations 2.36 and 2.40 into 2.35.

$$\left(1 - \frac{1}{n}\right) = \frac{\delta}{\varepsilon_i} \left[ \frac{\varepsilon_s}{L_{nw}} + \frac{qN_{sb}}{n} \right] \quad (41)$$

and from this equation

$$n = 1 + \frac{\delta}{\varepsilon_i} \left[ \frac{\varepsilon_s}{L_w} + qN_{sb} \right] \quad (2.42)$$

### 2.3.5 Cheung Functions and Determining Characteristics of Schottky Diode

Cheung came up with a new model to calculate Schottky diode parameters due to benefit from the forward bias of I-V characteristics of metal-semiconductor

contacts. If the current density from thermionic emission theory is multiplied by the area of the diode, the net current passing through the diode is obtained;

$$I = A \times J = \left[ AA^* T^2 \exp\left(\frac{-e\Phi_{bn}}{kT}\right) \right] \left[ \exp\left(\frac{eV_a}{kT}\right) - 1 \right] \quad (2.43)$$

Assume that  $eV_a \gg kT$ , so we can ignore 1. In practice, all applied voltage does not fall into the depletion region and there will be a deviation from the ideal condition. To express this deviation we should add a new term 'n' which is called ideality factor and it is unitless. Thus, the expression of current will be

$$I = A \times J = \left[ AA^* \exp\left(\frac{-e\Phi_{bn}}{kT}\right) \right] \left[ \exp\left(\frac{eV_a}{nkT}\right) \right] \quad (2.44)$$

In here the applied voltage will be dropped by  $IR_s$  which is called series resistance, so we should take  $V_a - IR_s$  instead of  $V_a$  and the new equation will be

$$I = A \times J = \left[ AA^* \exp\left(\frac{-e\Phi_{bn}}{kT}\right) \right] \left[ \exp\left(\frac{e(V_a - IR_s)}{nkT}\right) \right] \quad (2.45)$$

When we take the logarithm of the equation 2.45 and solve for  $V_a$ ,

$$V_a = \left(\frac{nkT}{e}\right) \ln\left(\frac{I}{AA^* T^2}\right) + n\Phi_{bn} + IR_s \quad (2.46)$$

is obtained. If the equation 2.46 is differentiated with respect to  $\ln I$

$$\frac{dV_a}{d(\ln I)} = \frac{nkT}{e} + IR_s \quad (2.47)$$

is obtained. The graph of the  $dV/d(\ln I)$  versus  $I$  in the equation is the linear and the slope of this line gives us  $R_s$ , series resistance. The ideality factor n is found from the interception point of this line with the vertical axis. The potential barrier height  $\Phi_{bn}$  can be defined as a function of  $H(I)$ ,

$$H(I) = V_a - \left(\frac{nkT}{e}\right) \ln\left(\frac{I}{AA^* T^2}\right) \quad (2.48)$$

From the equations 2.46 and 2.47 we can write  $H(I) = n\Phi_{bn} + IR_s$  and if we sketch the graph of  $H(I) - I$ , the slope of the line obtained gives us series resistance  $R_s$ . The barrier height  $e\Phi_{bn}$  can be found from the interception point of the line with  $H(I)$  axis.

### 2.3.6 The Schottky Capacity in the Metal-Semiconductor Schottky Diodes

The depletion region in the metal semiconductor contacts behaves as a capacitor with the space charges in the semiconductor side and the surface charges in the metal side. When the potential is increased in the state of the reverse bias, the width of the depletion region increases. If there is an important hole concentration near the metal, the hole concentration will decrease because of overlapping new Fermi energy level to the metal's Fermi energy level.

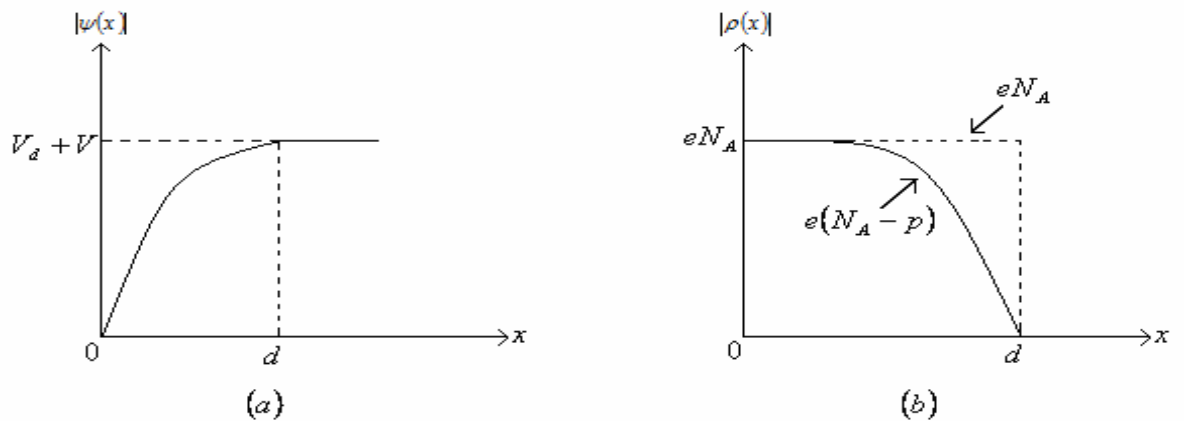


Figure 2.4 (a) potential distribution (b) Charge distribution of the metal/p-type rectifying contacts dependent to state.

The capacity of the Schottky region changes with the change in the charges. Thus, the Schottky diode can be used as a variable capacitor with voltage control. To find the Schottky region, the Poisson equation of the potential distribution at the barrier layer of the diode can be express as;

$$\nabla^2\psi(x) = \frac{d^2\psi}{dx^2} = \frac{\rho(x)}{\epsilon_s\epsilon_0} \quad (2.49)$$

where  $\epsilon_s$  is the dielectric constant of the semiconductor,  $\epsilon_0$  is the dielectric constant of the vacuum,  $\rho(x)$  is the space charge density dependent to the state. The space charge density can be written as ;

$$\rho(x) = e(N_a - N_d) \quad (2.50)$$

where  $N_d$  is the donor concentration of semiconductor,  $N_a$  is the acceptor concentration of semiconductor. The graphs of the potential function of  $\psi(x)$  and the space charge density  $\rho(x)$  dependent on the state are shown in Figure 2.4. Let assume ( $V_d$ ) represents the diffusion potential of the barrier layer and  $V$  represents the potential applied to the contact. As a result,  $N_d \gg n$ , since  $e(V_d - V) \gg kT$  in the  $0 \leq x \leq d$ . So, for n-type semiconductor we can write as;

$$\rho(x) \cong eN_a \quad (2.51)$$

When the equation 2.51 is used in Poisson equation;

$$\frac{d^2\psi}{dx^2} = -\frac{eN_a}{\epsilon_s\epsilon_0} \quad (2.52)$$

The condition states are looked for the last equation's solution ;

- 1) For  $x = 0$   $\psi(x) = 0$
- 2) For  $x > 0$   $\psi(x) = V_d + V$
- 3) For  $x = d$   $\frac{d\psi(x)}{dx} = 0$
- 4) For the equation 2.52, if we integrate by taking the third condition into consideration, we can obtain the electric field in the depletion region.

$$E(x) = -\frac{d\psi(x)}{dx} = -\frac{eN_a}{\epsilon_s\epsilon_0} (x - d) \quad (2.53)$$

by the integrating equation 2.53 under first condition,

$$\psi(x) = -\frac{eN_a}{\varepsilon_s\varepsilon_0} \left( \frac{1}{2}x^2 - xd \right) \quad (2.54)$$

If we solve this last equation with the second condition ;

$$d = \left[ \frac{2\varepsilon_s\varepsilon_0}{eN_a} (V_d \pm V) \right]^{\frac{1}{2}} \quad (2.55)$$

is obtained, and  $d$  is the width of the Schottky region. For  $V > 0$ , the contact is reverse bias and for  $V < 0$ , the contact is forward bias. The charge density for the semiconductor for the unit area is given by

$$Q = -eN_a d \quad (2.56)$$

By using 2.55 and 2.56 equations

$$Q = -[2\varepsilon_s\varepsilon_0 eN_a (V_d + V)]^{1/2} \quad (2.57)$$

is obtained. The Schottky capacity is defined as the exchange of the  $Q$  charge due to applied voltage which has the expression of (2.57). Hence, the capacity can be written as

$$C = \frac{\partial Q}{\partial V} \quad (2.58)$$

from the equations 2.57 and 2.58

$$C = \left[ \frac{\varepsilon_s\varepsilon_0 eN_a}{2(V_d + V)} \right]^{1/2} \quad (2.59)$$

or

$$C = \frac{\varepsilon_s\varepsilon_0}{d} \quad (2.60)$$

is obtained. As seen, the capacity of the depletion region is inverse proportional to applied voltage and the width of the Schottky region and proportional to concentration of the acceptor atoms directly.

## 2.4 Ohmic Contacts

Ohmic contacts are a type of contact used in semiconductor fabrication. They are the most common variety of contact because of their versatility and wide application range. The defining aspect of ohmic contacts is their low and constant resistance to the passage of electricity, which means they can be adapted to many uses and devices.

Assume that ( $\phi_m < \phi_s$ ) when a metal and a semiconductor are connected to each other.  $\phi_m$  is the work function of the metal and  $\phi_s$  is the semiconductor's work function. Before the contact, the Fermi level of the semiconductor is lower from the metal's Fermi level by the value of  $\phi_s - \phi_m$ .

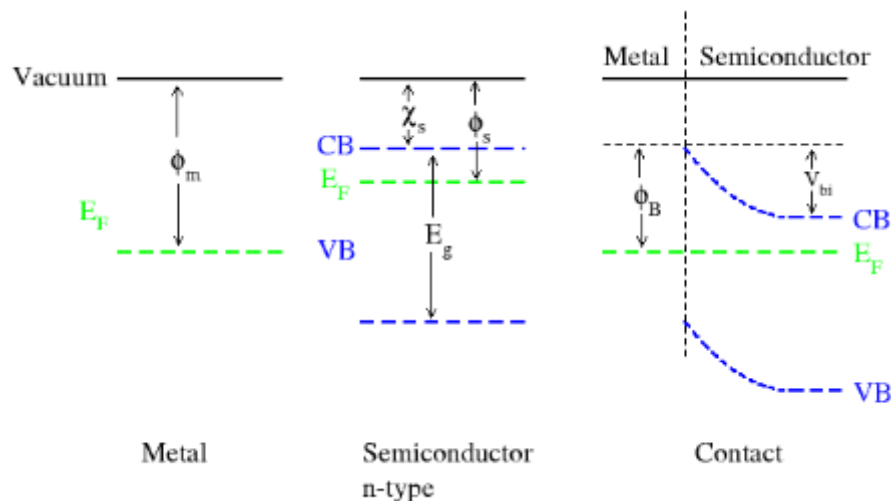


Figure 2.5 ( $\phi_m < \phi_s$ ) for this situation the energy band diagram of metal/n-type semiconductor ohmic contact.

After the establishment of contact, when the thermal equilibrium is achieved, the electrons flow from the metal to the semiconductor and therefore, the characterized property of n-type is increased at the surface of the semiconductor. These more electrons at the semiconductor's surface create a surface charge layer. And the electrons which are left from the metal, create a surface charge layer behind and thus a dipole layer occurs in the contact region.



If +V (voltage) is applied into the metal, there is no barrier for the electrons which flow from semiconductor to metal so the electrons move easily in this direction.

If +V (voltage) is applied into the semiconductor, electrons will meet very low potential barrier because of extremely doping state of the semiconductor and electrons easily flow from metal to the semiconductor. As a result in such a contact, the electrons move easily in both direction. This type of contact is called ohmic contact. When +V voltage is applied to the ohmic contact, the potential is dispersed over the whole body and when -V voltage is applied to the metal, this type contact is called injection contact because of that the transition of the electrons form metal to the conduction band of the semiconductor.

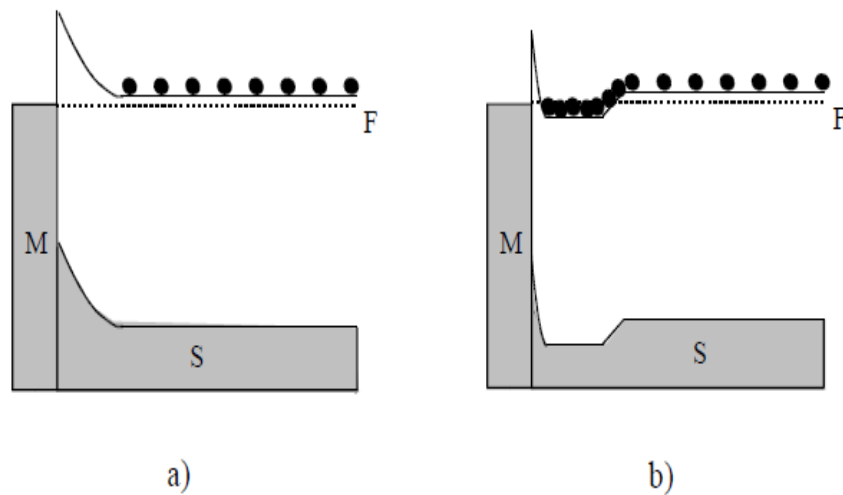


Figure 2.6 a) The barrier before doping. b) The barrier after doping. Black dots show us the conducting electrons.

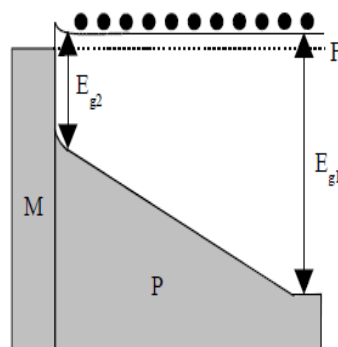


Figure 2.7 Decreasing of the Schottky barrier at the M-S junction in the case of an n-type graded-gap semiconductor. The band gap in the graded-gap semiconductor changes from  $E_{g1}$  to  $E_{g2}$ . Black dots show the conducting electrons.

Assume that  $\phi_m > \phi_s$  ( $\phi_m$  is the work function of metal,  $\phi_s$  is the work function of the semiconductor). The Fermi level of semiconductor is higher than the metal's Fermi level by the value of  $\phi_m - \phi_s$ . After contact, there will be a charge transporting. Electrons in semiconductor left a positive surface charge behind and these electrons flow into the metal and they constitute a negative surface charge in metal side. So that the Fermi energy level in semiconductor decreases by  $\phi_m - \phi_s$ . Surface of the semiconductor will be more p-type because of increasing in hole concentration. Electrons can pass through more easily from metal to the semiconductor to full up the empty states. This charge movement is the same as flowing holes from semiconductor to the metal. Holes passed metal are instantly ionized due to high electron concentration. In the reverse bias condition, holes in metal's conduction band which occur thermally can flow easily from semiconductor to metal. As a result in such a contact, the current move more easily to both direction. This type contacts are called as "ohmic contact".

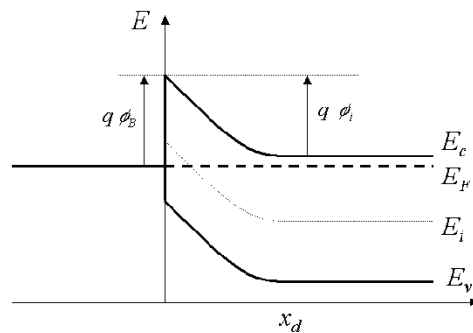


Figure:2.8 Energy band diagram for metal p-type semiconductor in thermal equilibrium after contact.

## CHAPTER 3

### EXPERIMENTAL PROCEDURE

#### 3.1 Introduction

In this chapter, first the techniques of electrodeposition is discussed and then how the substrate (n/Si ) is deposited with metal (chromium - Cr), also this chapter includes the steps of the preparing material and some cleaning process which is necessary to coat more sensitive.

#### 3.2 Electrodeposition Method

Electroplating is a plating process that uses electrical current to reduce cations on a conductive material to obtain a desired thickness of metal film. Electroplating is primarily used for depositing a layer of material to form some desired properties of metal films (e.g. abrasion and wear resistance, corrosion protection, lubricity, aesthetic qualities, etc.)

Abrasion is the effect of an abrasive scratches, removal of surface material.

Corrosion is the disintegration of an engineered material into its constituent atoms due to chemical reactions with its surroundings.

Lubricity is the process, or technique employed to reduce wear of one or both surface in close proximity, and moving relative to each other, by interposing a substance called lubricant between the surface to carry or to help carry the load (pressure generated) between the opposing surfaces. Another application uses electroplating to build up thickness on undersized parts.

In other words; electroplating is often also called “electrodeposition”, a short version of “electrolytic deposition”, and the two terms are used interchangeably. As a matter of fact; electroplating can be considered to occur by the process of electrodeposition.

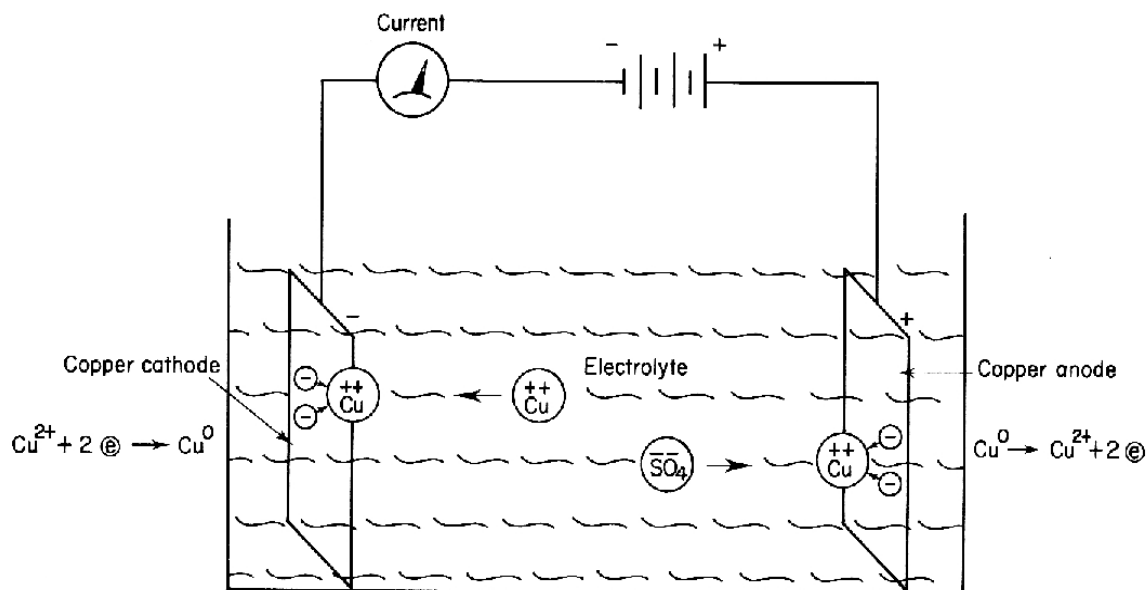
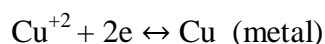


Figure 3.1. Electrolytic cell for the deposition of copper from copper sulphate solution.

Figure shows a simple electroplating system for the deposition of copper from copper sulphate solution.

The electrolytic solution contains positively charged ions (cations) and negatively charged sulphate ions (anions). Under the applied external electric field, the cations migrate to the cathode where they are discharged and deposit as metallic copper.



Copper from the anode dissolves into the solution to maintain the electrical neutrality.



The overall process is known as electrolysis. If some noble metal (such as platinum) is used as the anode, the overall reaction at the anode is oxidation of water.



The sulphate ions remain unchanged in quantity during the electrolysis. However, if noble metal is used as the anode, the concentration of Cu<sup>+2</sup> ions will decrease and that of H<sup>+</sup> ions will increase with time. Under this situation, extra copper sulphate

must be added into the solution from time to time and the hydrogen ions must be removed by neutralization with an alkali or by using a buffering solution.

In practical electrodeposition processes, the chemical reaction around the electrode area occurs in a more complicated way than that shown in figure 3.1.

Under the influence of an applied potential, rearrangement of ions near the electrode surface results in an electrical double layer called “Helmholtz double layer”, followed by the formation of a diffusion layer as shown figure 3.2.

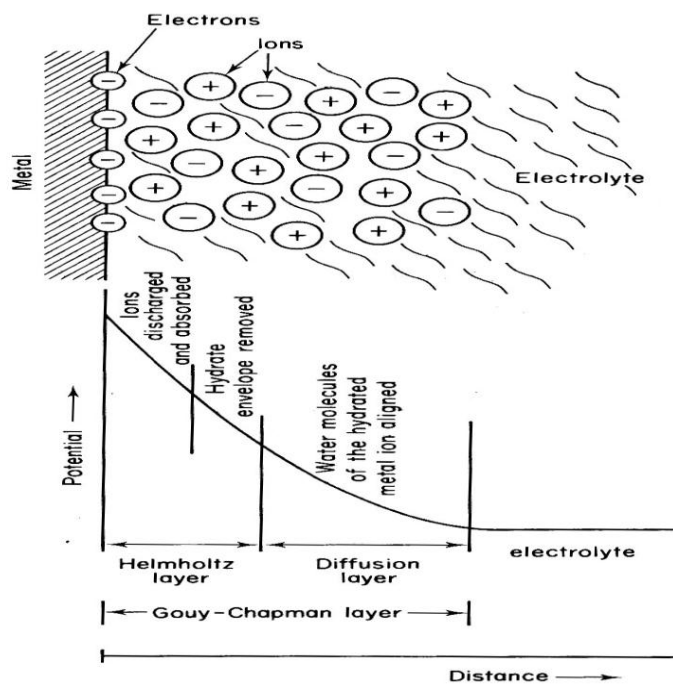


Figure 3.2. Electrical double layer

These two layers are referred as Gouy-Chapman layer. The process is as follows:

**Migration:** The hydrated metal ions in the solution migrate towards the cathode under the influence of impressed current as well as by diffusion and convection.

**Electron transfer:** At the cathode surface a hydrated metal ion enters the diffused double layer where the water molecules of the hydrated ion are aligned. Then the metal ion enters the Helmholtz double layer where it is deprived of its hydrate envelope.

**The dehydrated ion** is neutralized and adsorbed on the cathode surface.

**The adsorbed atom** then migrates or diffuses to the growth point on the cathode surface.

Thickness of the electroplated layer on the substrate is determined by the time duration of the plating. In other words, the longer the time the object remains in the operating plating bath, the thicker the resulting electroplated layer will be. Typically, layer thicknesses may vary with the using of Faraday's law. So it can be calculated easily and efficiently. An electroplated layer usually composed of a single metallic element. Co-deposition of two or more metal is possible under suitable conditions of potential and polarization, such as a Cu-Zn alloy or a Au-Sn alloy.

### 3.2.1 Experimental Set up of Electrodeposition System

Faraday concluded after several experiments on electrical current in non-spontaneous process that, the mass of the products yielded on the electrodes was proportional to the value of current supplied to the cell, the length of time the current existed, and the molar mass of the substance analyzed. In other words, the amount of a substance deposited on each electrode of an electrolytic cell is directly proportional to the quantity of electricity passed through the cell. This law explains that the thickness of the thin film, as in the following expression;

$$G/A = jtE\alpha \quad (\text{g cm}^{-2}) \quad (3.1)$$

In here,  $G/A$  is mass deposited per unit area,  $j$  is the current density,  $t$  is the time and  $\alpha$  is the current efficiency which is the ratio of the experimental to theoretical weight deposited and  $E$  is electric field. This equation can be written in a slightly different form to give the rate of deposition. If a thickness  $L$  is deposited in time  $t$ , then the rate of deposition  $L/t$  is given by

$$L/t = (j E \alpha) / \rho \quad (\text{cm/sec}) \quad (3.2)$$

where  $\rho$  is the film density.

Our system is checked by computer during the electrodeposition process to provide a constant current or constant potential for a certain period.

### 3.3 Growth Mechanism of the Thin Films by Electrodeposition Method

Metalization or metal deposition on semiconductor is an important role in the electronics industry [41-44] as it is a key step in many applications.

When an electrical potential is applied between a conducting area on the substrate and a counter electrode (usually platinum) in the liquid, a chemical redox process takes place resulting in the formation of a layer of material on the substrate. There are several factors in electrodeposition influence the performance and quality of the produced semiconducting thin films[45].

These factors can be ;

- The properties of substrate
- Current density
- The pH value of solution
- Solution temperature
- The composition of solution
- Deposition time
- Striking rate
- The applied potential or current during deposition process.

### 3.4 Preparation of the Substrate

The *n*-type Si wafer used in this study was (100) oriented and with free carrier concentration of  $1.25 \times 10^{15} \text{ cm}^{-3}$  from the reverse bias  $C^{-2}$ - $V$  characteristics at room temperature. The wafers were chemically cleaned using the RCA cleaning procedure as follows:

- a 10 min boil in  $\text{NH}_4\text{OH} + \text{H}_2\text{O}_2 + 6\text{H}_2\text{O}$ .
- a 10 min boil in  $\text{HCl} + \text{H}_2\text{O}_2 + 6\text{H}_2\text{O}$ .
- The native oxide on the front surface of the substrates was removed in  $\text{HF}:\text{H}_2\text{O}(1:10)$  solution.
- the wafer was rinsed in de-ionized water for 30 s.

### 3.5 Production of Schottky Diodes

Firstly, the matt side of the substrate is made an ohmic contact. For this, the heater is washed with % 10 HCl, and cleaned with deionized water and then dried. After that, it is placed in vacuum vaporization unit and then fired. Then, the Silicon wafers are cleaned chemically in RCA process and the material (the alloy of Au % 99- Sb % 1) which are used to make ohmic contact on the matt side of the wafer, is cleaned and placed into the crucible in the evaporator. After a vacuum of  $10^{-5}$  torr in the evaporation chamber is maintained, the evaporation of the alloy of Au-Sb is carried out. After the evaporation process, the Silicon wafer with Au-Sb is annealed at  $420^{\circ}\text{C}$  in an oven for 3 minutes. The schematic diagram of the oven used for the annealing process is shown in Figure 3.3.

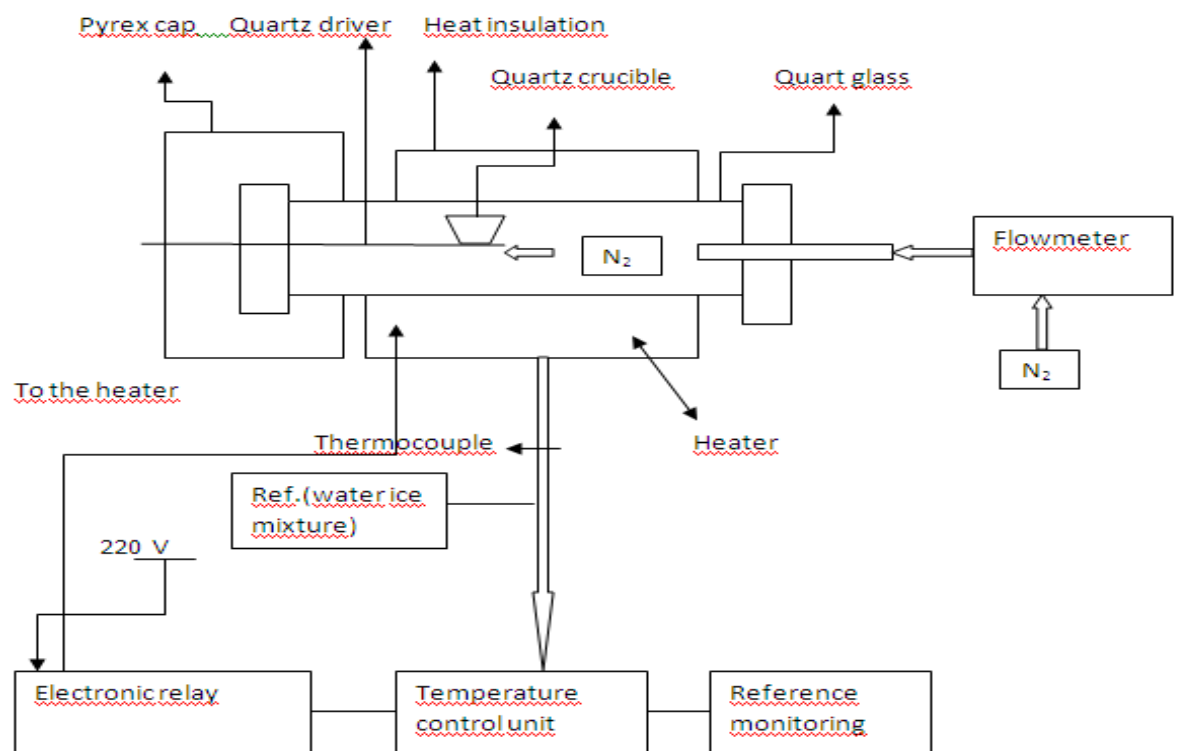


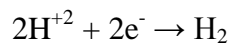
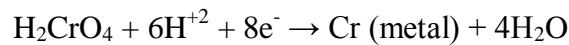
Figure 3.3 The diagram of the oven and control unit for the ohmic contact thermal process.



### 3.6 The development of the Chromium Layer on the n-type Silicon Wafer

The Schottky contacts were formed on the front shiny side of the n-Si as dots with diameter of about 1 mm by the galvanostatic electrodeposition of Cr. Adhesive tape which is resistant to acid was used to cover all the substrate except for the deposition area. The electrodeposition of Cr Schottky contacts on the n-Si substrate was carried out in galvanostatic mode from an electrolyte containing  $\text{CrO}_3$  (250g/l) and  $\text{H}_2\text{SO}_4$  (2.5 g/l) at room temperature. A Pt plate was used as anode while the n-Si substrate was connected as cathode. A current density of  $100\text{mA}/\text{cm}^2$  was maintained between the two electrodes. Film thickness was adjusted as 150nm by deposition time.

When  $\text{CrO}_3$  and  $\text{H}_2\text{SO}_4$  are dissolved in water, the solution contains positively charged ions of  $\text{Cr}^{+6}$  and  $\text{H}^+$  (cations) and negatively charged sulphate ions  $\text{SO}_4^{-2}$  (anions). Chromic acid  $\text{H}_2\text{CrO}_4$  is formed in the electrolyte. When an external electric field is applied between the cathode(n-Si) and the anode(Pt), the cations migrate to the cathode surface where chromium is reduced as Cr (metal), and hydrogen ions are discharged and released as  $\text{H}_2$  (gas). The presence of  $\text{SO}_4^{-2}$  ions in the electrolyte increases the adhesion ability of Cr ions and makes their deposition easier onto the Si substrate. The reactions which take place at the cathode (n-Si) surface are as follows:



## CHAPTER 4

### MEASUREMENTS AND RESULTS

#### 4.1. Measurement Techniques

In this section, the electrodeposited Chromium-n-type Si Schottky barrier and ideality factor are characterized. In the electrical characterization of these diodes, the current-voltage (I-V), capacitance-voltage (C-V) measurements are carried out.

The current-voltage (I-V) characteristics were measured using a Keithley 487 Picoammeter/Voltage Source in the wide temperature range (80-320 K) by steps of 20 K. Capacitance-Voltage characteristics were measured using a HP model 4192A LF impedance analyser in the wide temperature range (80-320K) by steps of 20 K.



Figure 4.1 Keithley 487 Picoammeter/Voltage Source

### 4.1.1. Current-Voltage Measurement

The schematic representation of the structure of the metal-semiconductor junction which consists of a metal contacting a piece of semiconductor and the sign convection of the applied voltage and current are shown in Figure 4.1, where  $x_d$  is the depletion layer width.

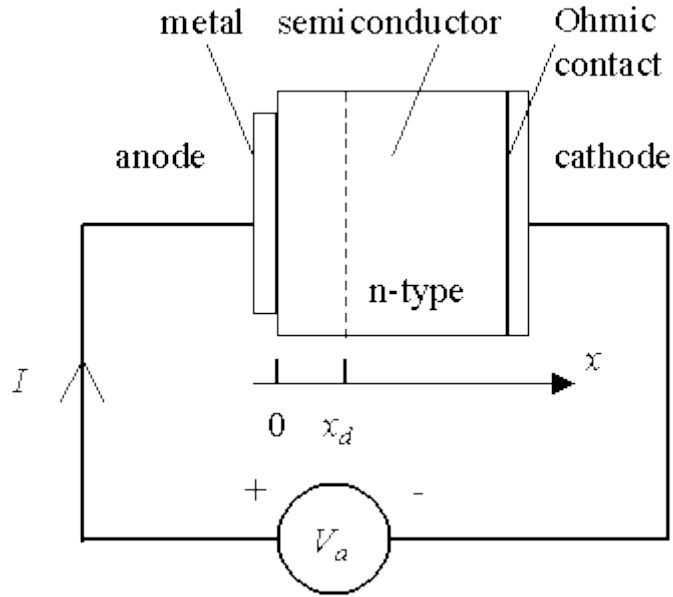


Figure 4.2 Structure and sign convection of a metal-semiconductor junction

The I-V characteristic in the forward direction with  $V = 3kT/q$  for relatively doped semiconductors is given by

$$J = A^{**}T^2 \exp\left(-\frac{q\Phi_{bn}}{kT}\right) \left[ \exp\left(\frac{qV}{kT}\right) - 1 \right] \quad (4.1)$$

From this equation

$$J = A^{**}T^2 \exp\left(-\frac{q\Phi_{b0}}{kT}\right) \left[ \exp(q(\Delta\Phi + V)/kT) \right] \quad (4.2)$$

where,  $A^{**}$  is the Richardson constant,  $\Delta\Phi$  is the image force lowering and  $\Phi_{b0}$  is the zero-field asymmetric barrier height. The ideality factor  $n$  is given by

$$n = \frac{q}{kT} \frac{\partial V}{\partial (\ln J)} \quad (4.3)$$

and

$$\Phi_{bn} = \frac{kT}{q} \ln \left( \frac{A^{**}T^2}{J_s} \right) \quad (4.4)$$

The major effect in the reverse direction is the Schottky-barrier lowering with  $V_R > 3kT/q$  and this reverse current component is the edge leakage current which is brought about the sharp edge around the border of the metal plate. This shows a resemblance with the junction curvature effect.

$$J_R \cong J_S = A^{**}T^2 \exp \left( -\frac{q\Phi_{bn}}{kT} \right) \exp \left( +\frac{q\sqrt{q\varepsilon/4\pi\varepsilon_s}}{kT} \right) \quad (4.5)$$

The reverse leakage current can be measured and plotted as a function of diode parameter [46]. If the barrier height  $q\Phi_{bn}$  is smaller than band gap so that the recombination-generation current in the depletion region is small with the Schottky emission current which increases slowly with the reverse bias as given by equation 4.5.

#### 4.1.2 Capacitance- Voltage Measurement

We can also calculate the barrier height with using capacitance measurements. If a small ac voltage is integrated with a dc bias, charges of one sign are induced on the metal surface incrementally and the opposite charges in the semiconductor. The correlation between capacitance (C) and voltage (V) is written as

$$C \equiv \frac{\partial Q_{SC}}{\partial v} = \sqrt{\frac{q\varepsilon_s N_D}{2(V_{bi} - V - \frac{kT}{q})}} = \frac{\varepsilon_s}{W} \quad (\text{farad/cm}^2) \quad (4.6)$$

and

$$\Phi_{bn} = V_{bi} + V_n + \frac{kT}{q} - \Delta\Phi \quad (4.7)$$

where,  $Q_{SC}$  is the space charge density per unit area of the semiconductor, C is the depletion region capacitance per unit area,  $\Delta\Phi$  is the Schottky barrier lowering,  $N_D$  is the doping concentration of n-type semiconductor, W is the width of the depletion region, V is the voltage and  $V_n$  is the depth of the Fermi level below the conduction band which can be obtained if the concentration of the doped semiconductor is known [47].

## CHAPTER 5

### RESULTS AND DISCUSSION

#### 5.1 Current-Voltage Measurement Results of the Schottky Diodes

The *n*-type Si wafer used in this study was (100) oriented and with free carrier concentration of  $1.25 \times 10^{15} \text{ cm}^{-3}$  from the reverse bias  $C^2$ - $V$  characteristics at room temperature which has a thickness of 150 nm and a mobility ( $\mu_n$ ) of  $1450 \text{ cm}^2/\text{V}\cdot\text{sec}$ .

To determine the donor density and Fermi level:

$$N_D = 1/q\mu_n\rho \quad (5.1)$$

$$N_D = N_C \exp(-E_F/kT) \quad (5.2)$$

The electrical characterizations of the devices were obtained through  $I$ - $V$  and  $C$ - $V$  measurements in the temperature range of 80-320 K by steps of 20 K. Thermionic emission (TE) theory explains the current flow mechanism across the metal-semiconductor interface in ideal conditions. According to TE theory [3-5], the current in Schottky contacts can be expressed as

$$I = I_o \exp\left(\frac{qV}{nkT}\right) \left[1 - \exp\left(-\frac{qV}{kT}\right)\right] \quad (5.3)$$

where  $I_o$  is saturation current derived from the straight line intercept of  $\ln I$  at zero bias and is given by

$$I_o = AA^*T^2 \exp\left(-\frac{q\Phi_{bo}}{kT}\right) \quad (5.4)$$

Where  $q$  is the electron charge,  $V$  is the definite forward-bias voltage,  $A$  is the effective diode area,  $k$  is the Boltzmann constant,  $T$  is the absolute temperature,  $A^*$  is the Richardson constant of  $112 \text{ A cm}^{-2} \text{ K}^{-2}$  for *n*-type Si [3,5, 48],  $\Phi_{bo}$  is the effective barrier height at zero bias (which is defined by Eq. (5.4)), and  $n$  is an ideality factor which is a measure of conformity of the diode to pure thermionic emission. The

ideality factor is obtained from the slope of the linear region of the forward bias  $\ln I$ - $V$  plot and can be written from equation (5.3) as

$$n = \frac{q}{kT} \frac{dV}{d(\ln I)} \quad (5.5)$$

The ideality factor, which is introduced to take into account the deviation of the experimental  $I$ - $V$  data from the ideal thermionic emission model, is close to unity in relative high temperature region what is characteristic for an ideal Schottky diode. The reverse and forward bias  $I$ - $V$  plots of the Cr/ $n$ -type Si Schottky contacts in the temperature range of 80-320 K are given in Figure 5.1.

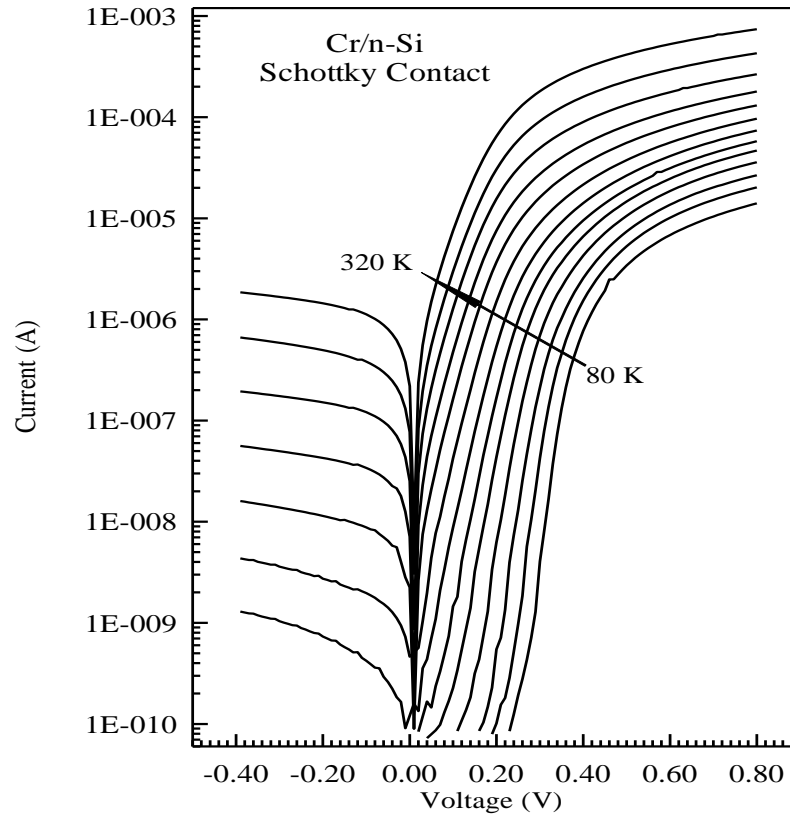


Figure 5.1 Current-voltage characteristics of the Cr/ $n$ -Si Schottky contact at various temperatures.

The experimental values of  $\Phi_{bo}$  and  $n$  were determined from equations (5.3) and (5.4), respectively, and are shown in Table 1 and Figure 5.2. As seen in Table 1 and Figure 5.2, the values of zero-bias barrier height  $\Phi_{bo}$  and  $n$  for the Cr/ $n$ -type Si Schottky contacts range from 0.316 eV and 2.257 (at 80 K) to 0.689 eV and 1.211 (at

320 K), respectively. Both parameters strongly depend on temperature. While  $n$  decreases,  $\Phi_{bo}$  increases with increasing temperature. Also, the values of barrier height obtained from Norde method which is described below, are given in Table 5.1.

Table 5.1 Temperature dependent values of various experimental parameters obtained from  $I$ - $V$  and  $C$ - $V$  measurements of the Cr/ $n$ -Si Schottky contact.

$T$ (K)	$I_o$ (A)	$N$ (IV)	$\Phi_{bo}$ (IV)	$\Phi_{bo}$ (eV) (Norde)	$\Phi_b$ (eV) (CV)	$nT$ (K)	$R_s$ (Norde) ( $k\Omega$ )
80	$1.99 \times 10^{-17}$	2.257	0.316	0.492	1.098	180.56	138.937
100	$1.89 \times 10^{-17}$	1.622	0.399	0.509	1.074	162.20	41.6322
120	$1.15 \times 10^{-15}$	1.494	0.441	0.528	1.059	179.28	38.818
140	$1.47 \times 10^{-14}$	1.423	0.487	0.544	1.024	199.22	29.312
160	$1.34 \times 10^{-12}$	1.398	0.498	0.56	0.969	223.68	21.649
180	$1.39 \times 10^{-11}$	1.359	0.528	0.583	0.933	244.62	13.806
200	$1.18 \times 10^{-10}$	1.341	0.553	0.599	0.868	268.20	11.230
220	$7.61 \times 10^{-10}$	1.312	0.577	0.613	0.823	288.64	8.729
240	$3.9 \times 10^{-9}$	1.285	0.5991	0.631	0.797	308.40	5.098
260	$1.39 \times 10^{-8}$	1.266	0.624	0.649	0.770	329.16	3.343
280	$4.63 \times 10^{-8}$	1.248	0.647	0.671	0.743	349.44	1.720
300	$1.26 \times 10^{-7}$	1.218	0.671	0.691	0.725	365.40	0.942
320	$3.79 \times 10^{-7}$	1.211	0.689	0.707	0.725	387.52	0.466

The mean barrier heights obtained from both plots are appropriate with each other. The values of  $\Phi_{bo}$  increase with increasing temperature, in which there is a positive coefficient that is in contrast to the negative dependence of coefficient for  $n$ -type Si [3,5]. This is likely due to the laterally inhomogeneous barrier height causing deviations from thermionic emission which becomes more pronounced as the

temperature decreases [5, 49, and 50]. Because the electrons possess a weak kinetic energy  $kT$  at low temperature, they prefer to pass the low barriers [50,51]. Since the current transport across the MS interface is a temperature-activated process at low temperatures, it will be dominated by current flowing through the patches of the lower SBH and larger ideality factor. The dominant BH will increase with the increasing temperature and bias voltage [4, 6, 22, 36, 39]. Furthermore, an apparent increase in ideality factors and decrease in barrier heights at low temperatures are possibly caused by some other effects (inhomogeneities of interface layer thickness and non-uniformity of the interfacial charges, etc.) giving rise to an extra current such that the overall characteristics still remain consistent with the TE process [52].

The capacitance-voltage ( $C$ - $V$ ) measurements are one of the most important non-destructive methods for obtaining information on rectifying Schottky contacts interfaces. Thus, the barrier height (BH)  $\Phi_{C-V}$  values at various temperatures for the Cr/ $n$ -type Si Schottky contact have been calculated from its experimental reverse bias  $C^2$ - $V$  characteristics given in Figure 5.3. The experimental values of  $\Phi_{C-V}$  as a function of the temperature are indicated by open squares in Figure 5.2; the  $\Phi_{C-V}$  values increased with increasing temperature. As can be seen in Table 5.1 and Figure 5.2, the  $\Phi_{C-V}$  values is higher than derived from  $I$ - $V$  measurements as expected. The experimental values of  $\Phi_{C-V}$  range from 1.098 eV at 80 K to 0.725 eV at 320 K. The discrepancy between  $\Phi_{CV}$  and  $\Phi_{IV}$  can be explained by the existence of excess capacitance and Schottky barrier height inhomogeneities [53-55]. The direct current across the interface is exponentially dependent on barrier height and the current is sensitive to barrier distribution at the interface. Whereas, the capacitance is insensitive to potential fluctuations on a length scale of less than the space charge width that the capacitance–voltage method averages over the whole area. Consequently, the barrier height values obtained from  $C$ – $V$  measurement is higher than that of barrier height values obtained  $I$ – $V$  measurements. Additionally, the discrepancy between the barrier height values of the devices may also be explained by the existence of an interfacial layer and trap states in semiconductor [3, 5, 56].



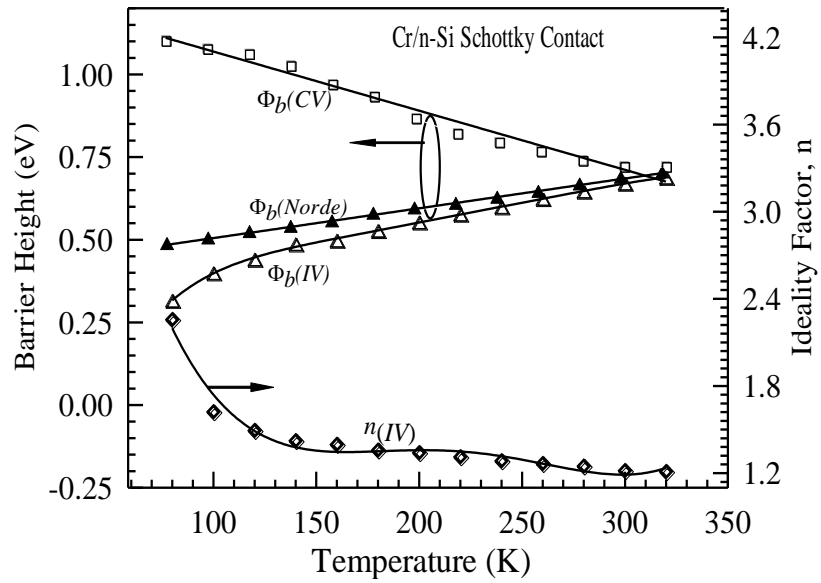


Figure 5.2 Temperature dependence of the ideality factor and barrier heights for Cr/n-Si Schottky contact.

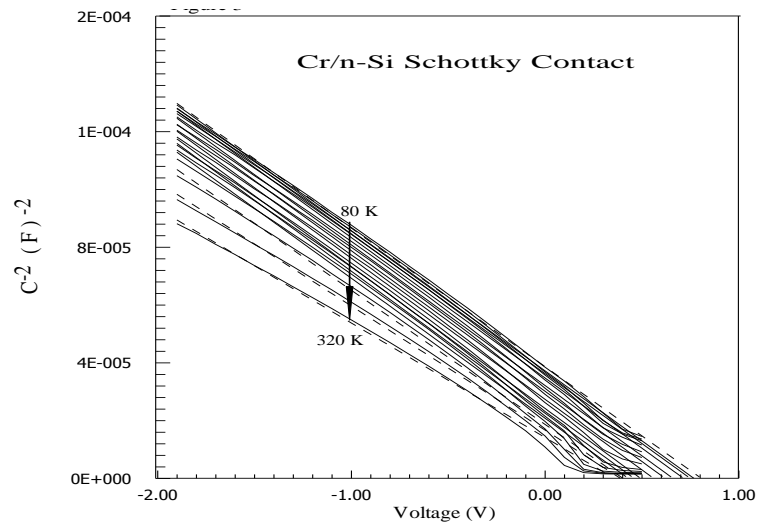


Figure 5.3 Experimental capacitance-voltage characteristics of a typical Cr/n-Si Schottky contact in the temperature range of 80-320K.

## 5.2 The $T_0$ effect

As explained above, the values of ideality factor,  $n$ , are not constant with temperature. The temperature dependency of the  $n$  can be more understood by a plot of  $nkT$  versus  $kT$ , such a plot is given for the Cr/n-type Si Schottky contact in Fig.4. As shown in Figure 5.4,  $n$  was found to be inversely proportional with temperature as  $n = n_0 + T_0/T$ , where  $n_0$  and  $T_0$  are a constant which were to be 1.03 and 57.28 K, respectively. The increase in ideality factor with decreasing temperature is known as  $T_0$  effect and is independent of temperature. This behaviour is typical of a real Schottky contact, i.e. a contact with a distribution of barrier inhomogeneities. In Figure 5.4, the dashed line presents the ideal behaviour,  $n=1$ , and the experimental data (open triangles) could be fitted by a straight line which is parallel to that of the ideal Schottky contact behaviour in the temperature ranges of 100-320 K. The deviation from linearity in the  $nkT$  vs.  $kT$  plot below 100 K is caused by the high value of the ideality factor,  $n$ , since the ideality factor is characterized by the current flow through the distribution of more low SBH patches at very low temperatures [38,57,58].

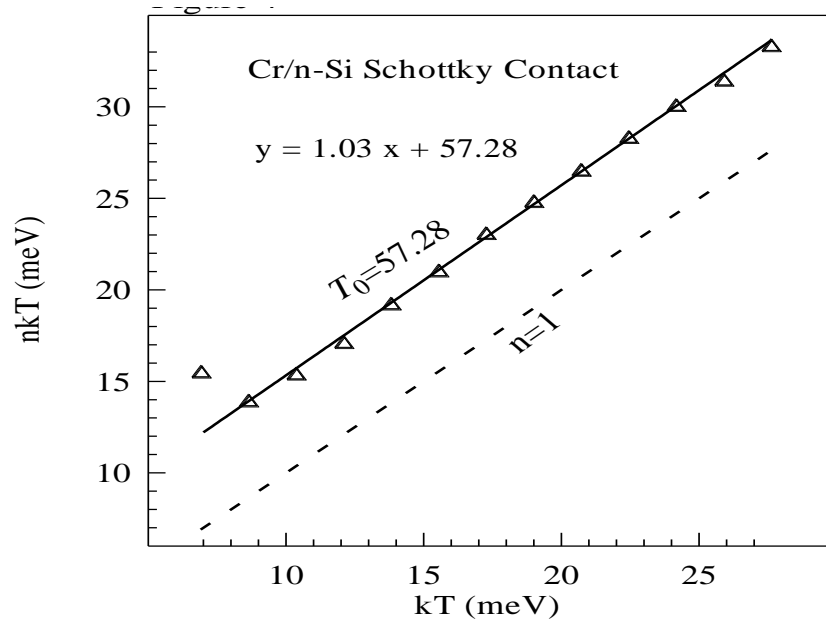


Figure 5.4 Plot of  $nkT$  as a function of  $kT$  showing the  $T_0$  anomaly from  $n = n_0 + (T_0/T)$ . The dashed line shows the ideal behaviour,  $n = 1$ . The open triangles are the experimental data in the temperature range of 80–320 K in Fig. 1. The value of the slope and the  $T_0$  are shown in the figure.

### 5.3 Inhomogeneous barrier analysis

The saturation current density for  $V=0$  used for the Richardson plot can be rewritten as;

$$\ln\left(\frac{I_o}{T^2}\right) = \ln(AA^*) - \frac{q\Phi_{bo}}{nkT} \quad (5.6)$$

where  $A^*$  is the Richardson constant and  $\Phi_{bo}$  is the mean zero voltage barrier height. Figure 5.5 shows the conventional Richardson plot. According to thermionic emission (TE) theory, the slope of the conventional Richardson plot [ $\ln(I_o/T^2)$  versus  $1/kT$  plot] should give the barrier height. However, the experimental data obtained do not correlate well with a straight line below 160 K. As will be discussed below, this behaviour has been interpreted on the basis of standard TE theory and the assumption of a Gaussian distribution of the barrier heights due to barrier inhomogeneities that persist at the metal-semiconductor interface. As can be seen in Figure 5.5, the conventional the  $\ln(I_o/T^2)$  versus  $1/kT$  Richardson plot is nonlinear. This nonlinearity in experimental  $\ln(I_o/T^2)$  versus  $1/kT$  curve may be caused by the temperature dependence of the BH and ideality factor, in particularly at lower temperature, due to the existence of the surface inhomogeneities of the Si substrate [3-7,10,13,18,24]. That is, the Richardson plots may be due to the spatially inhomogeneous BHs and potential fluctuations at the interface that consist of low and high barrier areas [4, 11, 12, 57-62]. Therefore, in the experimental  $\ln(I_o/T^2)$  versus  $1/kT$  curve, the Richardson constant value of  $A^* = 4.32 \times 10^{-5} \text{ A cm}^{-2} \text{ K}^{-2}$  is determined from the intercept at the ordinate of this experimental plot, which is much lower than the known value for holes in  $n$ -type Si ( $112 \text{ A cm}^{-2} \text{ K}^{-2}$ ). This deviation may be attributed to the spatial inhomogeneous barrier heights and potential fluctuations at the interface that consist of low and high barrier areas [4, 6, 14, 22, 36, 39, and 63]. Likewise, the dependence of  $\ln(I_o/T^2)$  versus  $1/nkT$  (open triangles) is linear in the temperature range 80–320 K with a slope giving an activation energy of 0.53 eV, and a value of Richardson constant ( $A^*$ ) obtained from the intercept at the ordinate is equal to  $4.65 \times 10^{-3} \text{ A cm}^{-2} \text{ K}^{-2}$ , which is still significantly lower than the known theoretical value of  $112 \text{ A cm}^{-2} \text{ K}^{-2}$  for  $n$  type Si [3,5]. As discussed above, the deviation in the Richardson plots may be due to the spatially inhomogeneous BHs and potential fluctuations at the interface that consist of low and high barrier areas that is, the current through the

diode will flow preferentially through the lower barriers in the potential distribution. As was explained by Horváth [36],  $A^*$  value obtained from the temperature dependence of the  $I$ - $V$  characteristics may be affected by the lateral inhomogeneity of the barrier, and the fact that it is different from the theoretical value may be connected to a value of the real effective mass that is different from the calculated one.

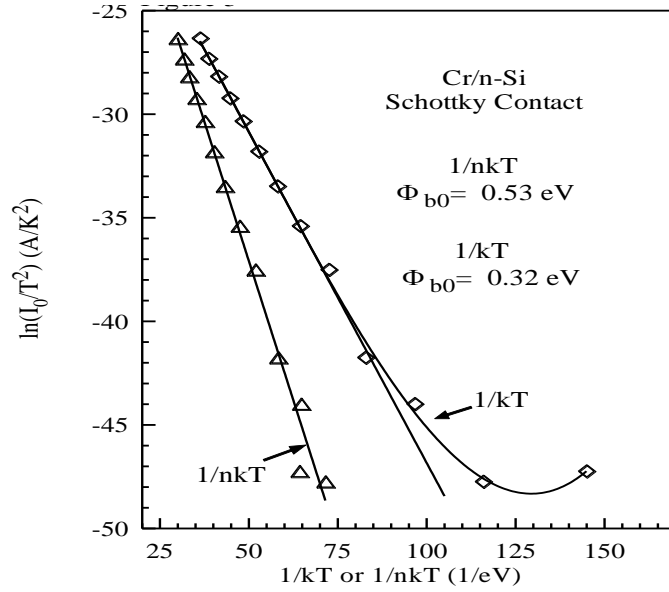


Figure 5.5 Conventional activation energy ( $\ln(I_0/T^2)$  versus  $1/kT$ ) plot (the open squares) and ( $\ln(I_0/T^2)$  versus  $1/nkT$ ) plot (the open triangles) for Cr/n-Si Schottky contact.

The significant decrease of the zero-bias BH and the increase in the ideality factor especially at low temperature is possibly caused by the BH inhomogeneities. Song et al [12] has introduced an analytical potential fluctuation model (a Gaussian distribution of the BHs). Now, the above abnormal behaviors can be explained using an analytical potential fluctuation model based on spatially inhomogeneous BHs at the interface [4, 11, 12, 22, 34, 63]. Let us assume that the distribution of the BHs is a Gaussian distribution of the BHs with a mean value  $\bar{\Phi}_b$  and a standard deviation  $\sigma_s$ . The standard deviation is a measure of the barrier homogeneity. The total current in a given forward bias  $V$  is then given by

$$I(V) = I_0 \exp\left(\frac{qV}{n_{ap}kT}\right) \left[1 - \exp\left(-\frac{qV}{kT}\right)\right] \quad (5.7)$$

with

$$I_0 = AA^*T^2 \exp\left(-\frac{q\Phi_{ap}}{kT}\right) \quad (5.8)$$

where  $\Phi_{ap}$  and  $n_{ap}$  are the apparent BH and apparent ideality factor, respectively, and are given by

$$\Phi_{ap} = \bar{\Phi}_{bo} - \frac{q\sigma_o^2}{2kT} \quad (5.9)$$

$$\left(\frac{1}{n_{ap}} - 1\right) = \rho_2 - \frac{q\rho_3}{2kT} \quad (5.10)$$

It is assumed that the mean SBH  $\bar{\Phi}_b$  and  $\sigma_s$  are linearly bias dependent on Gaussian parameters, such as  $\bar{\Phi}_b = \bar{\Phi}_{bo} + \rho_2V$  and standard deviation  $\sigma_s = \sigma_{so} + \rho_3V$ , where  $\rho_2$  and  $\rho_3$  are voltage coefficients which may depend on  $T$  and they quantify the voltage deformation of the BH distribution. The temperature dependence of  $\sigma_s$  is usually small and can be neglected. The experimental  $\Phi_{ap}$  versus  $1/T$  and  $1/n_{ap}$  versus  $1/T$  plots (Figure 5.6) drawn by means of the data obtained from Figure 5.1 respond to two lines instead of a single straight line with transition occurring at 180 K. Fitting of the experimental data in Eq.(5.4) or (5.8) and in Eq.(5.5) gives  $\Phi_{ap}$  and  $n_{ap}$ , respectively, which should obey Eqs. (5.9) and (5.10). Thus, the plot of  $\Phi_{ap}$  vs  $1/T$  (Figure 5.6) should be a straight line with the intercept at the ordinate determining the zero-bias mean barrier height  $\bar{\Phi}_{bo}$  and the slope giving the zero-bias standard deviation  $\sigma_s$ . The above observations indicate the presence of two Gaussian distributions of barrier heights in the contact area. The intercepts and slopes of these straight lines give two sets of values of  $\bar{\Phi}_{bo}$  and  $\sigma_s$  as 0.910 eV and 0.109 V in temperature range of 200-320 K (distribution 1), and as 0.693 eV 0.072 V in the temperature range of 80-180 K (distribution 2). As explained above, standard deviation is a measure of the barrier homogeneity. Thus, the lower value of  $\sigma_s$  corresponds to more homogeneous barrier height. However, it was seen that value of  $\sigma_s=0.109$  V is not small compared to the mean value of  $\bar{\Phi}_{bo}=0.910$  eV, and  $\sigma_s$

$=0.072$  V is not small compared to the mean value of  $\bar{\Phi}_{bo} = 0.693$  eV, too, so it indicates the presence of the interface inhomogeneities. This study shows that Cr/*n*-type Si Schottky contact has double-Gaussian distribution. The existence of a double-Gaussian in the metal–semiconductor contacts can be attributed to the nature of the inhomogeneities themselves in the two cases [32,34,64,65]. This may involve variation in the interface composition/phase, interface quality, electrical charges, non-stoichiometry, etc. They are important enough to electrically influence the  $I$ – $V$  characteristics of the Schottky contacts, at particularly low temperatures. Thus,  $I$ – $V$  measurements at very low temperatures are capable of revealing the nature of barrier inhomogeneities present in the contact area. That is, the existence of second Gaussian distribution at very low temperatures may possibly arise due to some phase change taking place on cooling below a certain temperature. Furthermore, the temperature range covered by each straight-line suggests the regime where corresponding distribution is effective [7].

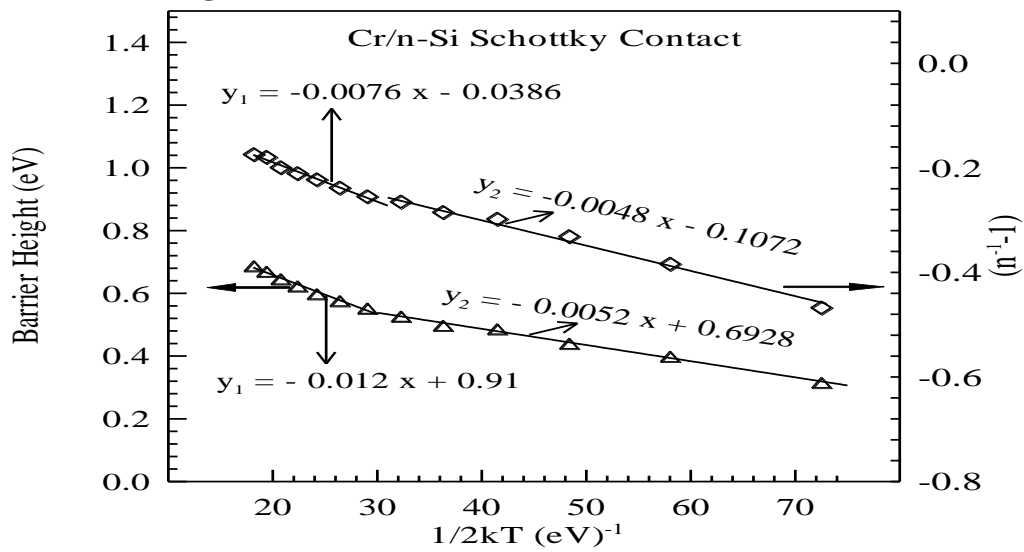


Figure 5.6 The barrier height  $\Phi_{ap}$  (the open triangles) obtained from  $I$ – $V$  measurements as a function of inverse temperature and the inverse ideality factor  $1/n_{ap}$  (the open squares) versus inverse temperature ( $1/2kT$ ) plot for Cr/*n*-Si Schottky contact.

Similarly the  $1/n_{ap}$  versus  $1/T$  should also possess different characteristics in the two temperature ranges if the contact contains two barrier height distributions. This is

indeed the case (open squares in Figure 5.6) as the data clearly fit with two straight lines in the temperature ranges 200-320 K and 80-180 K for Cr/n-type Si Schottky contact. The intercept and slope of the straight lines in  $1/n_{ap}$  versus  $1/T$  plot give the voltage coefficient  $\rho_2$  and  $\rho_3$ , respectively. The values of  $\Phi_2$  obtained from the intercepts of the experimental  $1/n_{ap}$  versus  $1/T$  plot (Figure 5.6) are 0.0386 V in the temperature range in 200–320 K (distribution 1), and 0.1072 in the temperature range in 80–180 K (distribution 2), whereas the values of  $\rho_3$  from the slopes are -0.0076 V in 200–320 K range and -0.0048 V in 80–180 K temperature ranges. The linear behaviour of this plot demonstrates that the ideality factor does indeed express the voltage deformation of the Gaussian distribution of the BH. As can be seen from the  $1/n_{ap}$  versus  $1/T$  plot,  $\rho_3$  value or the slope of the distribution 1 is larger than that of the distribution 2. Therefore, we may point out that distribution 1 is a wider and relatively higher barrier height with bias coefficients  $\rho_2$  and  $\rho_3$  being smaller and larger, respectively. Consequently, we can say that the distribution 2 at low temperatures may possible arise due to some phase change taking place on cooling below a certain temperatures.

Moreover, the activation energy plot,  $[(\ln(I_0/T^2))$  versus  $1/kT$  ], shows nonlinearity at low temperatures. To explain these discrepancies according to the Gaussian distribution of the BH, equation (5.8) can be rewritten by combining with equation (5.9) as

$$\ln\left(\frac{I_0}{T^2}\right) - \left(\frac{q^2 \sigma_s^2}{2k^2 T^2}\right) = \ln(AA^*) - \frac{q\bar{\Phi}_{bo}}{kT} \quad (5.11)$$

and a modified activation energy plot is made. For this, the term  $\ln(I_0/T^2) - q^2 \sigma_o^2 / 2k^2 T^2$  is calculated for both values of  $\sigma_s$ , associated with the Gaussian distributions of barrier heights, found above and then plotted as a function of inverse temperature in the temperature ranges of 80–180 K and 200–320 K. As can be seen, the values of  $\bar{\Phi}_{bo} = 0.66$  eV (in the range of 80–180 K) and 1.07 eV (in the range of 200–320 K) obtained from in Figure 5.7 are in close agreement with the  $\bar{\Phi}_{bo}$  obtained from the  $\bar{\Phi}_{ap}$  versus  $1/2kT$  plot in Figure 5.6. Likewise, the mean BH values obtained from Figures 5.5, 5.6, and 5.7 in high temperature ranges are very close to the BH values obtained from  $C^2$ - $V$  characteristics. This indicates that the BH measured by  $C$ - $V$  is

always close to the weighed arithmetic average of the Schottky barrier heights in the inhomogeneous metal- semiconductor contacts.

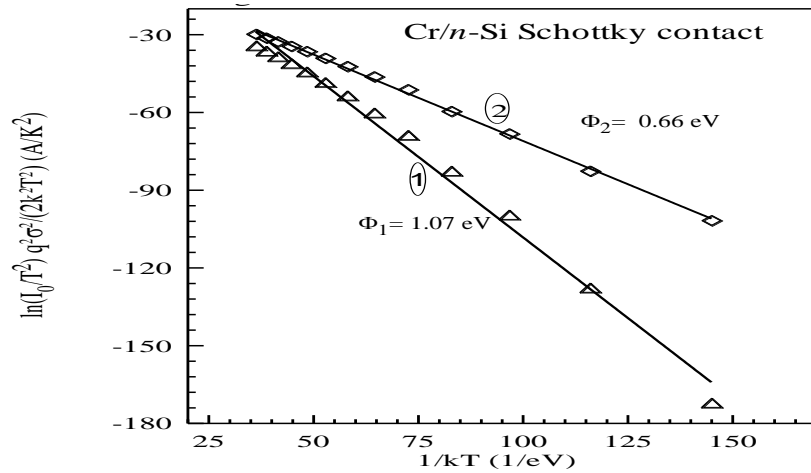


Figure 5.7 Modified activation energy ( $\ln(I_0/T^2) - q^2 \sigma_o^2 / 2k^2T$  versus  $1/kT$ ) plots for Cr/n-Si Schottky contact according to two Gaussian distributions of barrier heights. The plots for zero-bias standard deviation  $\sigma_s$  equal to 0.109 V and 0.072 V are shown by open triangles and open squares, respectively. The straight lines 1 and 2 indicate the best fitting of the data in the temperature ranges 200-320 K and 80-180 K, respectively.

#### 5.4 Norde's Function for the Series Resistance Calculation

It has been observed that the voltage drop caused a non-ideal behaviour at all temperatures at a high voltage region, which this region is series resistance region. According to the TE theory, the forward bias  $I$ - $V$  characteristics of a SBD with the series resistance can be expressed as [1,3]

$$I = I_o \exp\left(\frac{q(V - IR_s)}{nkT}\right) \quad (5.12)$$

where  $R_s$  is the series resistance and the  $IR_s$  term is the voltage drop across the series resistance of the diode. Norde proposed an alternative method to determine values of the series resistance and barrier height [58]. The following function (Norde's function,  $F(V)$ ) has been defined in the modified Norde's method [58]:

$$F(V) = \frac{V}{\gamma} - \frac{kT}{q} \ln\left(\frac{I(V)}{AA^*T^2}\right) \quad (5.13)$$

where  $\gamma$  is a first integer (dimensionless) greater than  $n$ , and  $I(V)$  is the current obtained from the current-voltage curve. Once the minimum of the  $F$  vs.  $V$  plot is



determined, the value of barrier height can be obtained from Eq. (5.14), where  $F(V_0)$  is the minimum point of  $F(V)$ , and  $V_0$  is the corresponding voltage:

$$\Phi_b = F(V_{\min}) + \frac{V_{\min}}{2} - \frac{kT}{q} \quad (5.14)$$

where  $F(V_{\min})$  is the minimum value of  $F(V)$ ,  $V_{\min}$  is the corresponding voltage. A plot of  $F(V)$  versus  $V$  for the Cr/*n*-Si Schottky contact at different temperatures is shown in Figure 5.8. According to Eq. (5.14), the barrier height values obtained by the Norde's method for the Cr/*n*-Si Schottky contact is given in Figure.5.2 (indicated by closed triangles). As can be seen in Figure 5.2 and Table 1, the BHs obtained by Norde's method are in good agreement with the values obtained by the  $I$ - $V$  method. The increase in the BHs at higher temperatures may be due to the interface states and chemical reactions between metal and semiconductor at the interface. As explained above, to compare the effective Schottky barrier height of contacts, the Norde method was also employed [66] because high series resistance ( $R_s$ ) can hinder an accurate evaluation of barrier height from the standard  $\ln I$ - $V$  plot. The value of the series resistance can be obtained from Norde's method for Cr/*n*-type Si Schottky structure. From Norde's functions the value of the  $R_s$  is determined as [66, 67]:

$$R_s = \frac{(2-n)kT}{qI_{\min}} \quad (5.15)$$

where  $I_{\min}$  is the corresponding current at  $V=V_{\min}$  where the function  $F(V)$  exhibits a minimum. From the  $F(V)$ - $V$  plots, the values of the series resistance ( $R_s$ ) of the Cr/*n*-type Si Schottky contact given in Figure. 5.9 and Table 1 have been determined as 0.466 k $\Omega$  at 320 K and 138.937 k $\Omega$  at 80 K, respectively. As can be seen in Table 1, the SBH has decreased and the series resistance has increased with decreasing temperature. The increase of the Cr/*n*-type Si Schottky contact resistivity causes an increase of  $R_s$ , which leads to a downward  $I$ - $V$  curve at high voltages. That is, when the temperature increases, more and more electrons have sufficient energy to surmount the higher barrier. Consequently, the dominant barrier height will increase with the temperature and bias voltage. The high values of the series resistance can be attributed to the freeze-out of carriers at low temperatures.

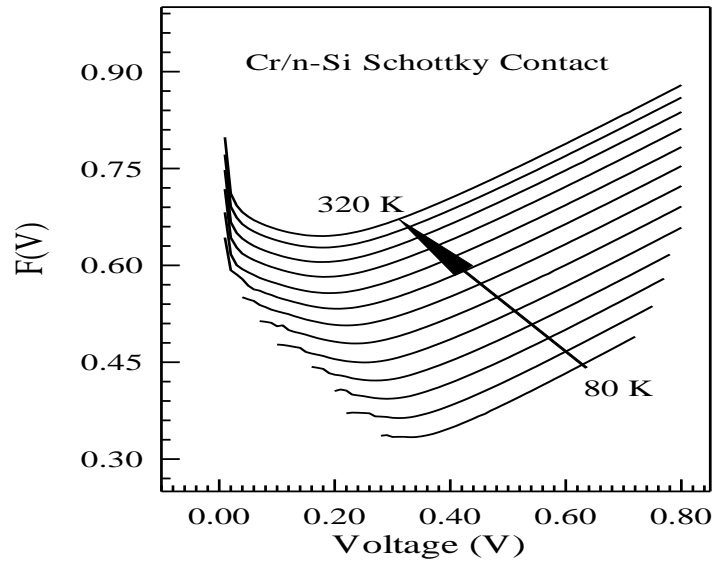


Figure 5.8  $F(V)$  versus  $V$  plot of the Cr/ $n$ -Si Schottky contact at various temperature.

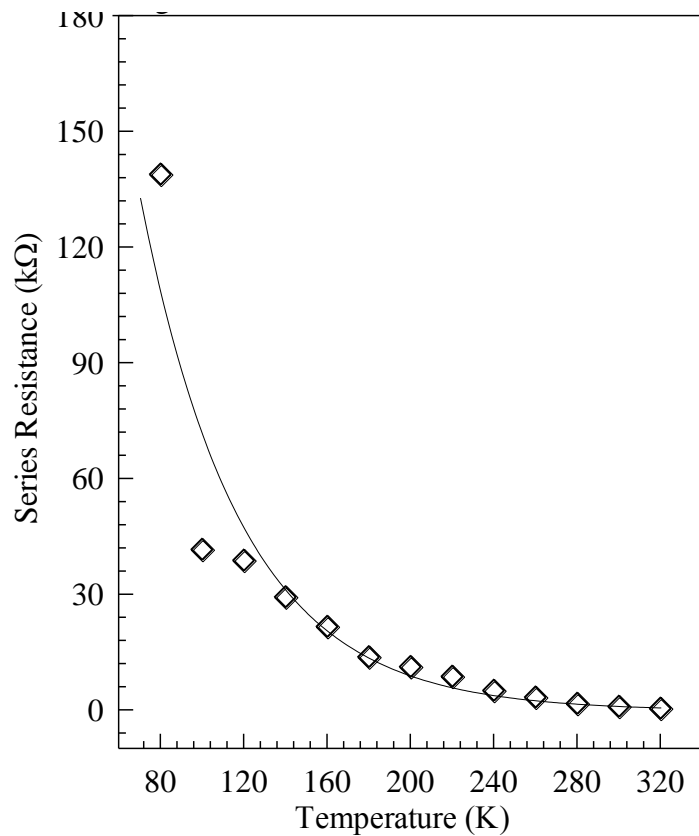


Figure 5.9 Temperature dependence of the series resistance from the Norde's functions of Cr/ $n$ -Si Schottky contact.

## CHAPTER 6

### CONCLUSION

In this study, the  $I$ - $V$  and  $C$ - $V$  characteristics of the Cr/ $n$ -Si Schottky contact were investigated in the temperature range of 80–320 K. The basic diode parameters such as ideality factor and barrier height were extracted from electrical measurements. The estimated barrier height  $\Phi_{bo}$  and the ideality factor  $n$  assuming thermionic emission mechanism show strong temperature dependence. It was seen that the ideality factor increased and the barrier height decreased with decreasing temperature. These results were ascribed to the barrier inhomogeneity at the metal/semiconductor interface. The electrical measurements were shown that the temperature-dependent current-voltage characteristics of the Cr/ $n$ -Si Schottky contacts can be explained by the double Gaussian distribution of barrier heights. The activation energy  $\ln(I_0/T^2)$  versus  $1/nkT$  plot yielded a straight line with an effective barrier height value 0.53 eV. It has been seen that the Gaussian distribution of BH model or  $n$  versus  $1/T$  plot show two slope behaviour and serve as the basis for the proposal of the presence of a double Gaussian distribution of BHs at the MS interface.

The modified  $\ln(I_0/T^2) - q^2 \sigma_o^2 / 2k^2 T^2$  versus  $1/kT$  plots yielded zero bias mean BH  $\bar{\Phi}_{bo}$  of 0.66 eV in the range of 80–180K (distribution 2) and 1.07 eV in the range of 200–320K (distribution 1). These values are in close agreement with the mean BHs obtained from the  $\Phi_{ap}$  versus  $1/2kT$  plot in Figure 5.6. In addition, the series resistance and barrier height values calculated with the Norde's method, and seen that the BHs obtained by the Norde's method are in good agreement with the values obtained by the  $I$ - $V$  method.

## REFERENCES

- [1] Liang, GR., Cui, TH. and Varahramyan, K. (2003) Fabrication and electrical characteristics of polymer-based Schottky diode. *Solid-State Electronics*, **47**, 691
- [2] Horvarth, Zsh., Adam, M., Szabo, I., Serenyi, M. and Van Tuyen, V. (2002) Modification of Al/Si interface and Schottky barrier height with chemical treatment. *Applied Surface Science*, **190**, 441
- [3] Sze, M. *Physics of Semiconductor Devices*, 2<sup>nd</sup> Edn.(Willey, New York 1981) p. 850.
- [4] Karataş, Ş., Altındal, Ş., Türüt, A., Özmen, A. (2003) Temperature dependence of characteristic parameters of the H-terminated Sn/p-Si(1 0 0) Schottky contacts. *Applied Surface Science*, **217**, 250.
- [5] Rhoderick, E.H. and Williams, R.H. *Metal-Semiconductor Contacts*, 2<sup>nd</sup> Edn. (Clarendon, Oxford, 1988).
- [6] Tung, R. T. (2001) Recent advances in Schottky barrier concepts, *Material Science and Engineering R*, **35**, 1-138.
- [7] Soylu, M. and Abay, B. (2009) Barrier characteristics of gold Schottky contacts on moderately doped n-InP based on temperature dependent I-V and C-V measurements. *Microelectronic Engineering* **86**, 88-95
- [8] Schmitsdorf, R.F., Mönch, W. (1999) Influence of the interface structure on the barrier height of homogeneous  $\text{Pb/n-Si(111)}$  Schottky contacts, *European Physical Journal B*, **7**, 457-466
- [9] Louis, E., Yndurain, F., Flores, F. Metal-semiconductor junction for (110) surfaces of zinc-blende compounds. *Physics Review B*, **13**, (1976) 4408
- [10] Heine, V. (1965) Theory of Surface States, *Physical Review* **138**, A1689-A1696

[11] Louie, S.G., Cohen, M. L. (1976) Electronic structure of a metal-semiconductor interface, *Physics Review B*, **13**, 2461

[12] Mc Cafferty, P.G., Sellai, A., Dawson, P., Elasd, H. (1996) Barrier characteristics of PtSi/*p*-Si Schottky diodes as determined from *I-V-T* measurements *Solid-State Electronics* **39**, 583.

[13] Chand, S., Kumar, J.(1996) Current-transport in Pd<sub>2</sub>Si/*n*-Si(100) Schottky barrier diodes at low temperatures. *Journal of Applied Physics A* **63**, 171-178.

Chand, S., Kumar (1997) Electron transport and barrier inhomogeneities in palladium silicide Schottkydiodes., *Journal of Applied Physics A* **65**, 497-593.

[14 ] Mamor, M, Sellai, A, Bouziane, K, Al Harthi, SH, Al Busaidi, M, Gard, FS. (2007) Model and experimental investigation of frequency conversion in AgGaGe<sub>x</sub>S<sub>2(1+x)</sub> ( $x = 0, 1$ ) crystals, *Journal of Physics D: Applied Physics* **40**, 1351.

[15] Asubay, S., Güllü, Ö., Türüt, A. (2009) Determination of the laterally homogeneous barrier height of metal/*p*-InP Schottky barrier diodes *Vacuum* **83** 1470–1474

[16] Lee, M. L., Sheu, J. K. and Lin, S. W. (2006) Schottky barrier heights of metal contactsto *n*-type gallium nitride with low-temperature-grown cap layer. *Applied Physics Letter* **88**, 032103

[17] Mamor, M. (2009) Analysis of Reverse-Bias Leakage Current Mechanisms in Metal/GaN Schottky Diodes. *Journal of Physics: Condensed Matter* **21**, 335802 (12pp)

[18] Dokme, I., Altindal, S., (2006) On the intersecting behavior of experimental forward bias current-voltage (*I-V*) characteristics of Al/SiO<sub>2</sub>/*p*-Si (MIS) Schottky diodes at low temperatures *Semiconductor Science and Technology* **21**, 81053.

[19] Karataş, Ş., Altindal, Ş. (2005) Analysis of *I-V* characteristics on Au/*n*-type GaAs Schottky structures in wide temperature range, *Material Science and Engineering B* 122-133.

- [20] Ayyildiz, E., Cetin, H., Horvath, Zs. (2005) Temperature dependent electrical characteristics of Sn/p-Si Schottky diodes, *Journal of Applied Surface Science* 252-1153.
- [21] Kılıçoğlu, T., Aydın, M.E., Topal, G., Ebeoğlu, M.A., Saygılı, H. (2007) The effect of a novel organic compound chiral macrocyclic tetraamide-I interfacial layer on the calculation of electrical characteristics of an Al/tetraamide-I/p-Si contact *Synthetic Metals* 157, 540–545
- [22] Werner, J.H., Güttler, H.H., (1991) Barrier Inhomogeneities at Schottky Contacts. *Journal of Applied Physics* 69, 1522-1533.
- [23] Chand, S., Kumar, J. (1997) Effects of barrier height distribution on the behavior of a Schottky diode *Journal of Applied Physics* 82, 5005.
- [24] Karataş, Ş., Altındal, Ş. (2005) Temperature dependent electrical characteristics of Sn/p-Si Schottky diodes. *Material Science and Engineering B* 122-133.
- [25] Kiziroglou, M E., Zhukov, A A., Abdelsalam, M., Li, X., de Groot, P A. J., Bartlett, P. N. and de Groot, C H. (2005) Electrodeposition of Ni-Si Schottky barriers. *IEEE Transactions on Magnetics* 41, 2639
- [26] Güler, G., Güllü, Ö., Bakkaloğlu, Ö.F., Türüt, A. (2008) Determination of lateral barrier height of identically prepared Ni/n-type Si Schottky barrier diodes by electrodeposition. *Physica B* 403, 2211–2214
- [27] Güler. G, Güllü. Ö, Karataş. Ş, Bakkaloğlu, Ö.F. (2009) Electrical Characteristics of Co/n-Si Schottky Barrier Diodes Using I-V and C-V Measurements. *Chinese Physics Letters* 26, 6, 067301
- [28] Forment, S., Van Meirhaeghe, R.L., De Vrieze, A., Strubbe, K., Gomes, W.P. (2001) A comparative study of electrochemically formed and vacuum-deposited n-GaAs/Au Schottky barriers using ballistic electron emission microscopy (BEEM). *Semiconductor Science and Technology* 16, 975.
- [29] Bao, Z.L., Kavanagha, K.L. (2006) Epitaxial Bi/GaAs diodes via electrodeposition, *Journal of Vacuum Science and Technology B* 24, 2138.

- [30] Eftekhari, A. (2003) Improving Cu metallization of Si by electrodeposition under centrifugal fields, *Microelectronic Engineering* **69**, 17.
- [31] Dokme, I., Altindal, S., Afandiyeva, I. M. (2008) The distribution of the barrier height in Al-TiW-Pd<sub>2</sub>Si/n-Si Schottky diodes from  $I-V-T$  measurements, *Semiconductor Science and Technology* **23**, 035003
- [32] Özdemir, A. F., Türüt, A., Kökçe, A. (2006) The double Gaussian distribution of barrier heights in Au/n-GaAs Schottky diodes from  $I-V-T$  characteristics, *Semiconductor Science and Technology* **21**, 298-302
- [33] Karataş, Ş., Çakar, M. (2009) Temperature dependence of the electrical and interface states of the Sn/Rhodamine-101/p-Si Schottky structures. *Synthetic Metals* **159**, 347–351
- [34] Chand, S., Kumar, J. (1995) Current-voltage characteristics and barrier parameters of Pd<sub>2</sub>Si/p-Si(111) Schottky diodes in a wide temperature range, *Journal of Semiconductor Science and Technology* **10**, 1680-1688
- Chand, S., Kumar, J. (1996) Evidence for the double distribution of barrier heights in Pd<sub>2</sub>Si/n-Si Schottky diodes from  $I - V - T$  measurements, *Journal of Semiconductor Science and Technology* **11**, 1203-1208
- Chand, S., Kumar, J. (1996) Current-transport in Pd<sub>2</sub>Si/n-Si(100) Schottky barrier diodes at low temperatures *Applied Physics A* **63**, 171
- [35] Aboelfotoh, M. O. (1991) Temperature Dependence of the Schottky-Barrier Height of Tungsten on n-Type and p-Type Silicon. *Solid State Electronics*. **34**, 51-55
- [36] Horvath, Zs. (1996) Analysis of I-V measurements on CrSi<sub>2</sub>-Si Schottky structures in a wide temperature range. *Journal of Solid State Electronics*. **39**, 176
- [37] Tamirci C. *Doktora Tezi*, Atatürk Üniversitesi Basımevi, ERZURUM.
- [38] Card, H.C. And Rhoderick, E.H., (1971) Studies of tunnel MOS diodes I. Interface effects in silicon Schottky diodes. *Journal of Physics D: Applied Physics* **4**,1589.

- [39] Türüt, A. And Sağlam, M., (1992) The determination of the density of Si-metal interface states and excess capacitance caused by them. *Physica B*, **179**,285
- [40] Andrews, J.M. and Leplester, M.P., (1970) Reverse Current-Voltage Characteristics of Metal-Silicide Schottky Diodes. *Solid State Electronics*, **13**, 1011.
- [41] Blum, W. (1952) 50 years of Electrochemical Theory. *Journal of Electrochemical Society*, **99**, 31C
- [42] Dettner, H.W., Elze, J. And Raub, E. (1966) *Handbuch der Galvanotechnik*. Carl Hanser Verlag, München.
- [43] McKinney, B.L. and Faust, C.L. J. (1977) Electron spin resonance and electrochemistry, *Electrochemical Society*, **124**, 379
- [44] Landolt, D. J. (2002) Electrodeposition Science and Technology in the Last Quarter of the Twentieth Century. *Electrochemical Society*, **149**, S9.
- [45] Bedir, M. (2002) Growth of Semiconducting and Conducting Thin Films and Investigation on Their Electrical, Magnetical and Optical Properties. *Thesis Ph. D. University of Gaziantep*.
- [46] Andrews J. M. and Koch, F. B. (1971) Formation of NiSi and Current Transport across the NiSi-Si interface, *Solid-State Electronics*., **14**, 901.
- [47] Sze, S.M. (1981). *Physics of Semiconductor Devices*. (2<sup>nd</sup> Edn.) New York: Wiley.
- [48] Güler, G., Güllü, Ö., Karataş, Ş., Bakkaloğlu, Ö.F. (2009) Analysis of the series resistance and interface state densities in metal semiconductor structures. *Journal of Physics: Conference Series* **153**, 012054
- [49] Aboelfotoh, M. O. (1989) Electrical characteristics of W-Si(100) Schottky barrier junctions, *Journal of Applied Physics* **66**, 262
- [50] Duman, S. (2008) Temperature dependence of current–voltage characteristics of an In/p-GaSe:Gd/Au–Sb Schottky barrier diode, *Semiconductor Science and Technology* **23**, 075042 (6pp)



- [51] Benmaza, H., Akkal, B., Abid, H., Bluet, J.M., Anani, M., Bensaad, Z. (2008) Barrier height inhomogeneities in a Ni/SiC-6H Schottky n-type , *Journal* **39**, 80
- [52] Altindal, Ş., Karadeniz, S., Tuğluoğlu, N., Tataroğlu, A. (2003) The role of interface states and series resistance on the I–V and C–V characteristics in Al/SnO<sub>2</sub>/p-Si Schottky diodes, *Solid-State Electronics*. **47**, 1847
- [53] Yakuphanoglu, F., Senkal, B.F. (2007) Electrical Characterization and Interface State Density Properties of the ITO/C<sub>70</sub>/Au Schottky Diode *Journal of Physical Chemistry C* **111**, 1840.
- [54] Chattopadhyay, S., Bera, L.K., Ray, S.K., Bose, P.K., Dentel, D., Kubler, L. J. L. Bischoff and C. K. Maiti, (1998) Determination of interface state density of Pt-Si/strained Si<sub>1-x</sub>Gex/Si Schottky diode characteristics, *Journal of Materials Science Materials in Electronics* **9**, 403.
- [55] Yakuphanoglu, F., Kandaz, M., Senkal, B.F. (2008) Current-Voltage and Capacitance Voltage Characteristics of Al / p-type silicon/organic semiconductor based on phthalocyanine rectifier contact. *Thin Solid Films* **516**, 8793–8796
- [56] Güllü, Ö., Biber, M., Türüt, A. (2008) Electrical characteristics and inhomogeneous barrier analysis of aniline green/p-Si heterojunctions, *Journal of Material Science: Material Electronics*. **19**, 986–991
- [57] Sullivan, J.P., Tung, R.T., Pinto, M.R., Graham, W.R. (1991) Electron transport of inhomogeneous Schottky barriers: A numerical study, *Journal of Applied Physics* **70**, 7403.
- [58] Tung, R.T. (1992) Electron transport at metal semiconductor interface: General Theory, *Physics Review B*. **45**, 13509.
- [59] Güllü, Ö., Biber, M., Duman, S., Türüt, A. (2007) Electrical characteristics of the hydrogen pre-annealed Au/n-GaAs Schottky barrier diodes as a function of temperature, *Applied Surface Science* **253**, 7246–7253
- [60] Osvald, J. (2003) New aspects of the temperature dependence of the current in inhomogeneous Schottky diodes, *Semiconductor Science and Technology* **18**, L24.

- [61] Zhu, S.Y., Van Meirhaeghe, R.L., Detavernier, C., Cardon, F., Ru, G.P., Qu, X.P. (2000) BEEM studies of the temperature dependence of Schottky barrier height distribution in CoSi<sub>2</sub>/n-Si(100) diodes formed by solid phase reaction. *Solid State Electron.* **44**, 663.
- [62] Ru, G.P., Van Meirhaeghe, R.L., Forment, S., Jiang, Y.L., Qu, X.P., Zhu, S., Li, B.Z. (2005) Voltage dependence of effective barrier height reduction in inhomogeneous Schottky diodes, *Solid State Electronics.* **49**, 606
- [63] Dimitruk, N.L., Borkovskaya, O.Yu., Dimitruk, I.N., Mamykin, S.V., Horvath, Zs. J., Mamontova, I.B. (2002) Morphology and interfacial properties of microrelief metal-semiconductor interface. *Applied Surface Science* **190**, 455
- [64] Altuntaş, H., Altındal, Ş., Shtrikman, H., Özçelik, S. (2009) A detailed study of current voltage characteristics in Au/SiO<sub>2</sub>/n-GaAs in wide temperature range. *Microelectronics Reliability* **49**, 904–911
- [65] Doğan, S., Duman, S., Gürbulak, B., Tüzemen, S., Morkoç, H. (2009) Temperature Variation of Current-Voltage Characteristics of Au/Ni/n-GaN Schottky Diodes, *Physica E- Low dimensional Systems and Nanostructures*, **41**, 646-651
- [66] Norde H. (1979) A modified forward I-V plot for Schottky diodes with high series resistance. *Journal of Applied Physics* **50**, 5052.